Title page

Title:

Context-specific functions of Notch in *Drosophila* blood cell progenitors

Running title:

Notch roles in blood cell progenitors

Names and affiliations of all authors:

Blanco-Obregon, DM[1*]; Katz, MJ[1,2*]; Durrieu, L[1,3]; Gándara, L[1,2]; Wappner, P[1,2,3**]

1. Instituto Leloir, CONICET, Patricias Argentinas 435, Buenos Aires (1405), Argentina.
2. Consejo Nacional de Investigaciones Científicas y Técnicas (CONICET), Buenos Aires, Argentina.
3. Departamento de Fisiología, Biología Molecular y Celular, Facultad de Ciencias Exactas y Naturales-Universidad de Buenos Aires, Buenos Aires (1428), Argentina.

* Contributed equally to this work.

**Corresponding author: pwappner@leloir.org.ar.

Key words:

Drosophila hematopoiesis; Blood cell progenitors; Notch signaling; Lymph gland

22 ## Summary statement

23 Notch signaling regulates differently distinct populations of blood cell progenitors of the
24 *Drosophila* larval hematopoietic organ.

Abstract

Drosophila Larval hematopoiesis takes place at the lymph gland, where myeloid-like progenitors differentiate into Plasmatocytes and Crystal Cells, under regulation of conserved signaling pathways. It has been established that the Notch pathway plays a specific role in Crystal Cell differentiation and maintenance. In mammalian hematopoiesis, the Notch pathway has been proposed to fulfill broader functions, including HSCs maintenance and cell fate decision in downstream progenitors. In this work we describe different roles that Notch plays in the lymph gland. We show that Notch, activated by its ligand Serrate, expressed at the Posterior Signaling Center, is required for Core Progenitor maintenance. We define a novel population of blood cell progenitors that we name Distal Progenitors, where Notch, activated by Serrate expressed in cells at the Medullary Zone/Cortical Zone boundary, regulates a binary decision between Plasmatocyte and Crystal Cell fates. Thus, Notch plays context-specific functions in different blood cell progenitor populations of the *Drosophila* lymph gland.

55 # Introduction

56 Hematopoiesis in *Drosophila* larvae takes place predominantly at the Lymph Gland (LG), which
57 is composed of two primary lobes symmetrically localized at both sides of the dorsal vessel, and
58 smaller posterior lobes that follow a similar array (1) (**Fig. 1a**). At the primary lobes, blood
59 progenitors (prohemocytes) differentiate into myeloid-like lineages through evolutionary
60 conserved mechanisms, making the LG an attractive model to explore the pathways involved in
61 normal and oncogenic hematopoiesis (2-4). At the 3rd larval instar, prohemocytes are compactly
62 arranged in an internal region of the primary lobe, called Medullary Zone (MZ), characterized by
63 the expression of the JAK/STAT receptor *domeless* (*dome*) (**Fig. 1a, b**) (1, 5, 6). Maturing
64 hemocytes are found in the peripheric region of the lobe, called Cortical Zone (CZ), which can
65 be identified by the expression of the Von Willebrand-like factor *hemolectin* (*hml*) (**Fig. 1a, b**)
66 (1). An Intermediate Progenitor (IP) population has been described at the MZ/CZ boundary,
67 defined by the expression of both *dome* and *hml* (**Fig. 1b**), but its physiological relevance
68 remains poorly defined (2, 7). Two types of differentiated populations of hemocytes occur at
69 the CZ: Plasmatocytes (PLs) and Crystal Cells (CCs) (**Fig. 1a**), whereas a third cell type, the
70 Lamellocytes, differentiate only following specific immune challenges. PLs, which constitute the
71 bulk (95%) of mature hemocytes, are macrophages that retain *hml* expression, while they also
72 express the receptors Nimrod (or P1-antigen) and Eater, both of them important for recognition
73 of bacteria (8-10). The CCs, named after their cytoplasmic inclusions of Prophenoloxydase
74 (ProPO), mediate melanization of pathogens and wounds, and constitute 5% of the total
75 number of mature hemocytes. Mature CCs are thus characterized by the expression of ProPO,
76 and no longer express the *hml* marker, characteristic of other CZ cells (5, 11). A population of
77 CC Progenitors can also be identified at the CZ by the expression of the RUNX transcription
78 factor Lozenge (Lz), homolog of the human AML1/Runx1 protein, frequently altered in Acute
79 Myeloid Leukemias (1, 12). Another remarkable LG region, termed Posterior Signaling Center
80 (PSC), occurs at the posterior tip of each primary lobe (**Fig. 1b**). It has been reported to function
81 as the niche that maintains the progenitor population of the MZ in an undifferentiated state
82 (13-15). PSC cells express the homeobox protein Antennapedia (Antp) (14), the signaling
83 molecule Hedgehog (Hh) (14), the Notch ligand Serrate (Ser) (16), and the gene *collier* (*col*),
84 ortholog of the mammalian Early B-cell Factor (EBF) (6, 17). Hh expressed at the PSC targets the
85 Medullary Zone and is required to restrain progenitor differentiation (14). Recently the notion
86 that the PSC functions as a hematopoietic niche has been challenged, as genetic ablation of this
87 structure did not alter progenitor maintenance nor steady-state blood cell differentiation (18,
88 19).

89 Notch is a conserved signaling pathway utilized repeatedly during development of all metazoa.
90 It is typically involved in cell differentiation, binary cell fate decisions, cell proliferation and cell
91 survival (20). The Notch receptor, which gives the name to the pathway, can be activated by its
92 transmembrane ligands Serrate (Ser) or Delta (Dl) expressed in adjacent cells (**Fig. 1c**). Once this
93 interaction takes place, Notch undergoes two consecutive cleavage events, resulting in the

release of the Notch Intracellular Domain (NICD), which migrates into the nucleus and binds the transcription factor Suppressor of Hairless (Su(H)). The complex formed by NICD and Su(H) recruits transcriptional co-activators, thereby inducing transcription of Notch target genes. This canonical Notch pathway was reported to operate in *hml*-positive cells of the Cortical Zone to specify the CC fate (16, 21, 22). The source of Notch ligand in this context is Serrate expressed at cells localized at the MZ/CZ boundary (16, 23). Non-canonical ligand-independent Notch signaling is afterwards required for CC maturation and survival (22).

In mammalian hematopoiesis, Notch pathway functions have been explored quite extensively, although with contrasting results. Notch receptors (Notch 1-4) are expressed in Hematopoietic Stem Cells, hematopoietic progenitors and mature blood cells, suggesting that Notch is required at multiple stages of the differentiation cascade (24). Notch functions in mammalian hematopoietic stem cells are controversial (25). Results in mouse models suggest that it is dispensable for their maintenance (26, 27), however *in vitro* conflicting evidences favoring either a function of Notch in HSC differentiation (28, 29), or a requirement for HSC maintenance have been reported (30-32). It is however well established that in lymphoid progenitors Notch promotes differentiation and proliferation of T lymphocytes at the expense of B lymphocytes (33, 34). Given the involvement of Notch in mammalian hematopoiesis, it is not surprising that alterations of this pathway are associated with several types of leukemia (35).

Because of the diverse, yet unclear functions of Notch in mammalian hematopoiesis, and given the conservation that occurs between the mechanisms controlling fly and mammalian blood cell development, we sought to explore the functions that the Notch pathway plays in *Drosophila* blood cell progenitors. We show here that Notch has distinct functions in two different populations of hemocyte progenitors: 1) In the recently described "Core progenitors" (36) Notch is required for maintenance of an undifferentiated state, a function that depends on Ser expressed at the PSC; and 2) In Distal Progenitors, a cell population defined in this paper, Notch controls a binary decision towards a PL or a CC fate. This binary Notch-dependent choice depends on Ser expressed in cells at the MZ/CZ boundary. Thus, Notch plays context-specific functions in two different cell progenitor populations during *Drosophila* hematopoiesis.

Results

Redefining progenitor cell populations of the Medullary Zone

Before analyzing Notch functions in *Drosophila* blood cell progenitors, we sought to define precisely the different populations of progenitors that occur at the MZ. Cells of the MZ of wandering 3rd instar larvae lymph glands express *domeMESO* and include a subpopulation of internal cells, the Core Progenitors, characterized by the expression of *tepIV* (36). It is unclear in the literature whether all *domeMESO*-expressing cells that are negative for *tepIV* coexpress *hml,* and can be considered Intermediate Progenitors. We found that this is not the case: In

131 larvae that coexpress the Blue Fluorescent Protein (BFP) under a *tepIV*-Gal4 driver (*tepIV* >
132 BFP), and GFP directly driven by a d*omeMESO* promoter (*domeMESO*-GFP), along with dsRed
133 controlled directly by an *hml* promoter (*hml*-dsRed), three distinct cell populations can be
134 recognized: 1) Core Progenitors positive for both *tepIV* > BFP and *domeMESO*-GFP (**Fig. 1d**,
135 region 1); 2) Cells positive only for *domeMESO*-GFP (**Fig. 1d**, region 2); and 3) Intermediate
136 Progenitors in which *domeMESO*-GFP and *hml*-dsRed signals overlap (**Fig. 1d**, region 3). Thus,
137 an uncharacterized population of *domeMESO* progenitors which do not express *tepIV* or *hml*
138 occurs in the lymph gland. We henceforth propose the name "Distal Progenitors" for this
139 particular population, in reference to their distal location from the dorsal vessel and Core
140 Progenitors. Interestingly, the membrane receptor Eater, often considered a PL-specific marker
141 (10, 37), is also expressed in Distal Progenitors of wandering 3rd instar larvae (**Fig. 1e**, region 2),
142 whereas it is barely detectable in Core Progenitors (**Fig. 1e**, region 1).

143 We conclude that three distinct populations of hemocyte progenitors occur at the Medullary
144 Zone of 3rd instar larvae lymph glands: 1) Core Progenitors, which co-express *tepIV* and
145 *domeMESO*; 2) Distal Progenitors that are positive for *domeMESO* but negative for *tepIV* and
146 *hml*; and 3) Intermediate Progenitors, which co-express *domeMESO* and *hml* (**Fig. 1f**).

147

148 ***The Notch pathway is required for Core Progenitor maintenance***

149 Notch expression is widespread throughout the lymph gland, suggesting that this pathway
150 might operate in various cell types (**Fig. 2a**, upper). We initially analyzed Notch function in Core
151 Progenitors by expressing a *notch* RNAi with *tepIV*-Gal4 (**Fig 2a**, middle), and observed a clear
152 reduction of Core Progenitors (**Fig. 2a, b**), while both Plasmatocytes (PLs) and Crystal Cells
153 (CCs), increased significantly (**Fig. 2b**). The number of cells of the PSC remained unaltered (**Fig.**
154 **S1a**). As mentioned above, in wandering 3rd instar larvae the receptor Eater is expressed in
155 Distal Progenitors, while it is almost undetectable in Core Progenitors, so we utilized Eater as
156 another marker to assess the effect of Notch on progenitor populations. Notch silencing with
157 *tepIV*-Gal4 resulted in a clear expansion of the *eater* expression domain (**Fig. 2c**), confirming
158 that Notch is necessary for Core Progenitor maintenance. Consistent with this, silencing of
159 another component of the canonical Notch pathway, the transcription factor Suppressor of
160 Hairless (Su(H)), also provoked a reduction of Core Progenitors, while PLs and CCs increased
161 significantly (**Fig. 2d**). Altogether, these results suggest that the Notch pathway is required cell-
162 autonomously for maintenance of Core Progenitors in an undifferentiated state.

163 We next analyzed whether over-activation of the Notch pathway provokes the opposite
164 phenotype, namely an increase of Core Progenitors and general differentiation impairment.
165 This was not the case, as over-expression with *tepIV*-Gal4 of a full-length Notch construct (**Fig.**
166 **S1b**) or Su(H) did not alter Core Progenitor, PL or CC populations (**Fig. S1c, d**). These results
167 suggest that endogenous activity of the Notch pathway is already sufficient to prevent
168 excessive differentiation of Core Progenitors. It was recently reported that Notch is expressed

169 transiently at the 1st larval instar (L1) in a small group of Hematopoietic Stem Cells (HSCs) (38),
170 so we analyzed the possibility that the phenotype that we observed in Core Progenitors stems
171 from an alteration of Notch function in L1 HSCs. To investigate this, we used a thermosensitive
172 Gal80 construct to silence Notch expression only from mid-second larval instar onwards (**Fig.**
173 **S1e**, upper). The results were identical to those in which Notch was constitutively silenced (**Fig.**
174 **S1e** and **Fig. 2b**), ruling out the possibility that the loss of Core Progenitors observed after
175 Notch silencing depends on an early role in L1 HSCs.

176 The findings shown in this section are consistent with a requirement of the Notch pathway for
177 maintenance of Core Progenitors in an undifferentiated state.

178

179 ***Serrate expressed at the Posterior Signaling Center is required for Core progenitor***
180 ***Maintenance***

181 As a next step, we studied the identity and source of the ligand for Notch activation in Core
182 Progenitors. *Serrate* (*ser*) is expressed at high levels in PSC cells (1, 14, 16, 23), although no
183 functions have been yet attributed to this expression. Since the PSC and Core Progenitors are in
184 close proximity, and filopodia that emanate from PSC cells may play a role in transmitting
185 signals to MZ progenitors (14), we asked whether Ser expressed at the PSC activates Notch for
186 Core Progenitor maintenance. First, we silenced Ser at the PSC with an *antp*-Gal4 driver, and
187 observed an increased number of PLs and CCs (**Fig. 3a**), indicating that Ser is required at the PSC
188 to limit differentiation. In line with this, analysis of *eater*-dsRed expression following *antp*-Gal4
189 dependent silencing of Ser revealed a clear reduction of Core Progenitors (*eater*-negative) (**Fig.**
190 **3b**). These results indicate that Ser is required specifically at the PSC for Core Progenitors
191 maintenance.

192 Recently, the notion that the PSC functions as a hematopoietic niche has been challenged, as
193 *antp*-Gal4 driven Reaper expression (i.e. apoptotic ablation of the PSC) did not alter PL or CC
194 differentiation (18). In that study, genetic ablation of the PSC was confirmed at L3 stage by the
195 lack of expression of two classical PSC markers, Hh and Antp, whereas Ser expression was not
196 assessed (18). We thus analyzed if *ser* expressing cells are still present in LGs in which the PSC
197 was genetically ablated. Ablation was induced from L2 stage onwards by using a Gal80
198 thermosensitive construct to prevent Reaper expression and lethality at earlier stages. We
199 monitored the expression of a *ser-LacZ* construct (1, 14, 16, 23, 39), and consistently observed
200 the presence of *ser*-expressing cells in LGs where *antp*-positive cells were ablated (**Fig 3c**,
201 lower). Importantly, in wild-type lymph glands we observed PSC cells that express *ser* but not
202 *antp* (**Fig. 3c**, upper), suggesting that the PSC might encompass a mixed population of cells, with
203 a large proportion of them co-expressing *antp* and *ser*, while some cells express *ser* but not
204 *antp*. These observations are consistent with a model in which, after genetic ablation of the
205 $antp^+$ cells of the PSC, the remaining ser^+, $antp^-$ PSC cells are sufficient to sustain normal Core
206 Progenitor maintenance and hemocyte differentiation. Noteworthy, after *antp*-driven ablation,

207 a negative correlation between surviving *ser*$^{+}$, *antp*$^{-}$ PSC cells and hemocyte differentiation
208 occurs: Lymph glands with a small *ser*-positive area at the PSC display greater PLs
209 differentiation than those with a larger *ser*-positive area at the PSC (**Fig. 3d**). These results
210 suggest that *ser* expressing cells of the PSC are important for Core Progenitor maintenance, and
211 that the *ser* expressing cells that survive to *antp*-driven apoptotic cell ablation can support
212 normal blood cell differentiation.

213

214 ***In Distal Progenitors the Notch pathway controls a binary cell fate decision***

215 We have shown above that *notch* silencing with *tepIV*-Gal4 provokes enhanced differentiation
216 of both PLs and CCs (**Fig. 2b**). In sharp contrast, *notch* silencing with *domeMESO*-Gal4 brought
217 about almost complete loss of CCs accompanied by an increased proportion of PLs (**Figs. 4a and**
218 **S2a**). Similar results were obtained when *su(H)* was silenced with the same driver (**Fig. 4b**),
219 suggesting that the Notch pathway promotes CC differentiation in Distal Progenitors, while the
220 PL fate is inhibited. To further explore this possibility, we over-expressed with *domeMESO*-Gal4
221 a full-length Notch construct (**Fig. S2b**) or the Notch Intracellular Domain (NICD), and observed
222 in both cases that PL differentiation was virtually blocked, and CCs increased dramatically (**Fig.**
223 **4c**). Over-expression of Su(H) with *domeMESO*-Gal4 provoked the same effect (**Fig. 4d**). We
224 thus conclude that an increase of Notch pathway activity in Distal Progenitors induces CC
225 differentiation and inhibits PL differentiation.

226 To confirm that the activity of Notch is indeed required for normal differentiation in Distal
227 Progenitors that are positive for *domeMESO* and negative for *hml* (**Fig. 1d, f**), *notch* silencing
228 with *domeMESO*-Gal4 was repeated in a genetic background in which *notch* RNAi expression in
229 cells that co-express *hml* was inhibited by QUAS-Gal80 (*domeMESO*-Gal4 > UAS-N^{RNAi}; *hml*-QF >
230 QUAS-Gal80). Silencing of Notch in this genetic background provoked identical effects to those
231 observed without expression of Gal80 in *hml*-positive cells (**Fig. S2c**). In a control experiment,
232 *hml*-QF driven expression of QUAS-Gal80 effectively repressed Gal4 activity in the CZ (**Fig. S2d**).
233 These results confirm that Notch operates in the Distal Progenitors, which express *domeMESO*
234 but not *hml*.

235 Together, this set of experiments indicates that in Distal Progenitors the Notch pathway
236 regulates a binary fate decision, promoting CC differentiation while inhibiting the PL fate.

237

238 ***Eater is an early Plasmatocyte fate marker in Distal Progenitors***

239 Next, we explored further aspects of this Notch-dependent binary fate decision that takes place
240 in Distal Progenitors. Noteworthy, a closer look to *eater*-dsRed reporter expression shown in
241 **Fig. 1e** revealed that *eater-dsRed* can be detected in most Distal Progenitors but is virtually
242 absent in a few cells within this region (**Fig. 5a**). A possible explanation is that *eater*-expressing
243 Distal Progenitors at the 3rd instar might be already committed towards a PL fate, while those

244 Distal Progenitors with very low *eater* levels are likely committed to become CCs. Consistent
245 with this notion, we observed at the CZ that *eater*-dsRed expression occurs in most *hml*-positive
246 cells, while it is excluded from those cells that express the CC progenitor marker Lz (**Fig. 5b**).
247 Lineage tracing experiments with an *eater*-Gal4 driver revealed that the lineage does not
248 include CCs (**Fig. 5c**), supporting that *eater* expression in Distal Progenitors marks a Distal
249 Progenitor subpopulation committed for a PL cell fate. *Eater*-Gal4 driven *notch* silencing or
250 Notch over-expression did not recapitulate the effects observed when *domeMESO*-Gal4 was
251 utilized to perform the same manipulations (compare **Figs. 4a, c** with **Fig. S3a**), suggesting that
252 Notch operates in Distal Progenitors that have not yet begun to express *eater*. The above
253 observations are consistent with a model in which, at an earlier developmental stage, *eater*-
254 negative uncommitted Distal Progenitors make the binary cell fate decision regulated by Notch,
255 while later, *eater* is expressed in cells committed to a PL fate.

256 If *eater* is indeed an early marker for Distal Progenitors committed to a PL fate, its expression
257 should be controlled by the Notch pathway. We assessed this possibility by over-expressing
258 Notch with *domeMESO*-Gal4, a treatment that induces massive differentiation to CCs (**Fig. 4c**),
259 and observed almost complete absence of *dome*$^+$, *eater*$^+$ double-positive Distal Progenitors (**Fig.**
260 **5d**). Conversely, Notch silencing provoked a complete conversion of *dome*$^+$ *eater* $^-$ progenitors
261 into *dome*$^+$, *eater*$^+$ double-positive Distal Progenitors (**Fig. 5d**). These observations suggest that
262 *eater* expressed in Distal Progenitors is an early marker for a Notch-dependent binary fate
263 decision, labeling cells committed to a PL fate.

264

265 ***Serrate expressed at the MZ/CZ boundary regulates the cell fate decision in Distal Progenitors***

266 Groups of Serrate-expressing cells lying next to the MZ/CZ boundary, which instruct progenitors
267 to acquire a CC fate have been previously reported (16, 23). We therefore investigated whether
268 these cells provide the ligand for the Notch-dependent binary cell fate decision in Distal
269 Progenitors. We noticed that a major proportion of these Ser-expressing cells, but not the Ser-
270 expressing cells of the PSC, co-express *domeMESO* (**Fig. 6a**), so we utilized *domeMESO*-Gal4 to
271 manipulate Ser expression. Silencing of *ser* with *domeMESO*-Gal4 virtually blocked CC
272 differentiation, while it increased PL proportion (**Fig. 6b**), mimicking the effect of *notch* silencing
273 with the same Gal4 driver (**Fig. 4a**). In agreement, overexpression of Ser rendered the opposite
274 results, increasing CCs and reducing PLs (**Fig. 6c**). Thus Ser expressed in cells of the MZ/CZ
275 boundary is required for Notch activation in Distal Progenitors, controlling the binary cell fate
276 choice. The E3 ubiquitin ligase *neutralized* (*neu*) is necessary for Ser endocytosis and Notch
277 activation in neighboring cells (40). Mimicking the results obtained after *ser* silencing with
278 *domeMESO*-Gal4, expression of a *neu* RNAi with the same driver reduced CC number and
279 increased PLs (**Fig. 6d**), further supporting the notion that Ser expressed at the MZ/CZ boundary
280 activates Notch signaling for the binary cell fate decision in Distal Progenitors.

281

282 # Discussion

283 In mammals, Notch receptors (Notch 1-4) are expressed in HSCs, hematopoietic progenitors
284 and mature blood cells, suggesting that Notch is required at multiple levels of blood cell
285 differentiation. Particularly, the role of the Notch pathway in HSC maintenance has been
286 explored in depth, although with contrasting results. Some experiments in cell culture suggest
287 that Notch is required for HSC maintenance (30-32), while others suggest that it promotes HSC
288 differentiation towards the myeloid lineage (28, 29). Works *in vivo* in which interactions with
289 the hematopoietic niche is still present, and therefore recapitulate better a physiologic
290 situation, also yielded conflicting results. Studies utilizing conditional knock-out mice affecting
291 different elements of the canonical Notch pathway suggested that Notch is dispensable for HSC
292 maintenance (26, 27), while others indicated that alterations of Notch signaling are associated
293 with development of myeloproliferative disease (MPD), characterized by accumulation of
294 mature cells of the myeloid lineage (41). Thus, the role of Notch in adult HSC homeostasis is at
295 least controversial and requires further examination. Many aspects of mammalian and
296 *Drosophila* hematopoiesis are conserved, particularly at the level of the transcription factors
297 and signaling pathways involved (2-4). One striking parallelism between *Drosophila* and
298 mammalian models is the expression in the hematopoietic niche of the Notch ligand Serrate
299 (Ser)/Jagged (JAG). While Ser is expressed in cells of the *Drosophila* PSC (16), mammalian JAG1
300 and JAG2 expression has been detected in different bone marrow cell types that fulfill niche
301 functions, including endothelial cells and cells of the hematopoietic stroma (42-44). The wide
302 array of genetic tools available in *Drosophila* allow for manipulations of gene expression with an
303 exquisite temporal and spatial specificity that is currently not possible to the same extent in
304 mammalian systems. Thus, the utilization of the fly model may provide clues for addressing
305 unresolved issues related to Notch functions in mammalian hematopoiesis.

306 In the current work, we have analyzed biological properties of *Drosophila* blood cell
307 progenitors. This analysis led us to redefine the progenitor subpopulations of the larval lymph
308 gland. A novel progenitor population, the "Distal Progenitors" that are positive for *domeMESO*
309 and negative for both *tepIV* and *hml,* occurs at the medullary zone. Our results strongly suggest
310 that the binary fate decision between PLs and CCs is made in naïve Distal Progenitors at early
311 larval stages, while later in development, at wandering 3rd instar larvae, the PL-specific marker
312 *eater* is expressed in most but not all Distal Progenitors, marking the cells that are already
313 committed to a PL fate. The remaining Distal Progenitors with low *eater* levels are committed to
314 become CCs, as suggested by *eater* lineage tracing, as well as by *eater* and Lz mutually exclusive
315 expression in *hml*-positive cells. Thus, the Medullary Zone, in wandering 3rd instar larvae,
316 encompasses an undifferentiated population of cells, the Core Progenitors, and a second
317 population, the Distal Progenitors, which have already been instructed to become either PLs or
318 CCs.

319 We have found that Notch, which is expressed throughout the lymph gland, plays distinct
320 functions in Core Progenitors or Distal Progenitors (**Fig. 7**). In Core Progenitors Notch is required

321 for maintenance of the undifferentiated state; our results thus contribute to the incipient
322 characterization of the Core Progenitor subpopulation, in which *collier* (*col*) is expressed at low
323 but physiologically relevant levels (36). We found that Notch function in Core Progenitors
324 depends on Ser that is expressed at the PSC. This Ser expression has been reported before (1,
325 14, 16, 23), but its function remained elusive. Filopodia emanating from PSC cells and
326 intermingling between cells of the MZ have been described, and were proposed to participate
327 in Hedgehog signaling (14). Given our observation that Ser expressed at the PSC is necessary for
328 Notch activation in Core Progenitors, and considering that direct cell-cell interactions are
329 required for Notch stimulation by its ligands, it seems reasonable to hypothesize that the
330 filopodia that emanate from the PSC may play a role in Notch signaling as well (6).

331 It has been shown that genetic ablation of the PSC by expression of the proapoptotic protein
332 Reaper (Rpr) does not alter Core Progenitor maintenance nor steady-state differentiation,
333 challenging the notion that the PSC functions as a hematopoietic niche (18). Using the same
334 PSC-ablation protocol with *antp*-Gal4 driven expression of Rpr from L2 stage onwards, we
335 detected the presence of *ser*-positive cells in the PSC that escaped genetic ablation. Moreover,
336 in wild-type lymph glands the PSC includes a subpopulation of cells that are *ser*-positive and
337 *antp*-negative (ser^{+}, $antp^{-}$). It is therefore likely that those *ser*-positive cells that survived *antp*-
338 Gal4 induced genetic ablation are responsible for maintaining Core Progenitors and for
339 sustaining normal progenitor differentiation.

340 We have found that in Distal Progenitors Notch fulfills a totally different function; it regulates a
341 binary cell fate decision, promoting CC differentiation, and inhibiting differentiation of PLs (**Fig.**
342 **7**). We propose that the activation of the Notch pathway in Distal Progenitors is achieved
343 through direct interaction of early naive Distal Progenitors with Ser-expressing cells localized at
344 the MZ/CZ boundary, thereby inducing CC differentiation and repressing the PL fate. On the
345 other hand, naive Distal Progenitors that do not contact these Ser-expressing cells undergo a
346 default differentiation program towards a PL fate (**Fig. 7**). Our finding that Notch regulates in
347 Distal Progenitors a binary cell fate decision between a PL and a CC fate is in line with previous
348 results by Tokusumi et al. (45): These authors utilized the allelic combination $su(H)^{1}/su(H)^{115B}$,
349 and observed a total block of CC differentiation accompanied by massive differentiation of PLs
350 that invaded the MZ. According to the model proposed in the current study (**Fig. 7**), this is
351 indeed the expected outcome of Tukusumi et al. experiments (45), where a combined effect of
352 Core Progenitor loss, along with inhibition of the CC fate and default differentiation towards the
353 PL fate in Distal Progenitors is expected. It is still an open issue whether early fate specification
354 in Distal Progenitors establishes the final (95:5) proportion of PLs versus CCs observed at the
355 Cortical Zone, or if alternatively, the fate specification in Distal Progenitors brings about an
356 initial 50:50 proportion of cells committed to one versus the other fate, followed by increased
357 proliferative capacity of PL-committed Distal Progenitors.

358 The Notch pathway has been previously demonstrated to be necessary and sufficient for CC
359 specification at the CZ (16, 21, 22). Our results suggest that Notch-dependent CC specification

occurs earlier in Distal Progenitors, and that Notch is probably required at later stages to sustain the original specification. Two works support this notion: Firsty, Krzemien et al. (46) utilized a clone labelling strategy at different larval stages, reaching the conclusion that blood cell progenitors of early L2 larvae, which have not yet developed a CZ, have already restrained their differentiating potential, either towards a PL or a CC fate. Secondly, at later stages of CC development, namely when Lz expression begins in unipotent CC progenitors at the CZ, it has been reported that Notch inhibits the expression of PL-specific genes (47). In this study, gene expression manipulations performed with *lz*-Gal4 demonstrated that the Notch target gene *klumpfuss* (*klu*) mediates repression of P1 expression in CC progenitors, thereby stabilizing CC commitment (47). We induced *klu* silencing with *domeMESO*-Gal4 in multipotent Distal Progenitors, and did not observe alterations of PL or CC differentiation (data not shown). This observation suggests that Notch target genes that regulate the early fate decision in Distal Progenitors, and those target genes that mediate CC-fate stabilization later at the CZ may be different. The identity of the Notch target genes that regulate initial cell fate determination in Distal Progenitors are not known and should be addressed in future investigations.

Notch function as a regulator of the cell fate choice in Distal Progenitors is remarkably similar to the role of Notch reported in the control of a binary cell fate decision in mammalian lymphoid progenitors (24, 33, 34, 48, 49). In this case, inhibition of the Notch pathway induces a default differentiation program towards a B lymphocyte fate, while the T lymphocyte fate is abolished (33, 34, 48). Conversely, over-activation of the Notch pathway induces a T cell fate, while B cell differentiation is inhibited (49). Even though *Drosophila* progenitors are considered myeloid-like lineage cells, this similarity in Notch-dependent blood progenitor cell fate decision with the mammalian lymphoid lineage suggests a primitive mechanism of cell communication that determines a balance of blood cell types in hematopoiesis.

The Notch pathway is therefore employed several times during hematopoiesis at the lymph gland. First: A possible role in HSC at the 1st larval instar (38); second: It is required for maintenance of Core Progenitors (this study); third: In Distal Progenitors it regulates the binary cell fate choice between PLs and CCs (this study); fourth: At the CZ, it is involved in fate stabilization in CC progenitors (47), and later it is required for CC maturation and survival (22). With the development of increasingly sophisticated genetic tools in mammalian systems, future studies may determine if Notch fulfills comparable context-specific functions throughout the mammalian hematopoietic hierarchy.

Materials and Methods

Fly Strains and crosses

The following *Drosophila* strains were used: *domeMESO*-GFP; *hml*-dsRed; *domeMESO*-Gal4; *antp*-Gal4 (U. Banerjee), *ser*-LacZ (A. Bachmann); *eater*-dsRed; *eater*-Gal4 (RA. Schulz). The

397 following stocks were obtained from the Bloomington Stock Center: UAS-GFP; UAS-BFP; *GFP*
398 RNAi; QUAS-GFP; QUAS-Gal80; *hml*-Gal4; *hml*-QF; *notch* RNAi; *notch* RNAi (2); *su(H)* RNAi; *tub*-
399 Gal80^{ts}; UAS-Su(H); UAS-Notch; UAS-NICD; *ser* RNAi; UAS-Ser; *neu* RNAi; UAS-RedStinger, UAS-
400 Flp, Ubi-p63E(FRT.STOP)Stinger (G-TRACE, (50)). *TepIV*-Gal4 was obtained from the Vienna
401 *Drosophila* Resource Center. All experimental crosses were performed at 25 ^{o}C and F1 larvae
402 were incubated at 29 ^{o}C to maximize Gal4 activity, with the exception of experiments involving
403 *tub*-Gal80^{ts}, in which larvae were kept at 18 ^{o}C and then transferred to 29 ^{o}C to induce Gal4
404 activity. Experiments involving *notch* RNAi (2) and *su(H)* RNAi were performed in a genetic
405 background that included UAS-Dicer2 to enhance silencing.

406 *Immunohistochemistry*

407 Lymph glands were processed and stained as previously described (5): lymph glands were
408 dissected from third-instar larvae (unless otherwise stated) in 1× PBS, fixed in 4%
409 formaldehyde/1× PBS for 30 min, washed three times in 1×PBS with 0.4% Triton-X (1× PBST) for
410 15 min each, blocked in 10% normal goat serum/1× PBST for 30 min, followed by incubation
411 with primary antibodies overnight at 4°C in blocking solution. Primary antibodies were washed
412 three times in 1× PBST for 15 min each, re-blocked for 30 min, followed by incubation with
413 secondary antibodies for 2 hr at room temperature. Samples were then washed three times in
414 1× PBST prior to mounting on glass slides in glycerol with Mowiol 4-88 anti-fade agent (EMD
415 Millipore Corp., Billerica, MA). The following primary antibodies were used: rabbit α-βgal
416 (Cappel), rabbit α-GFP (ThermoFisher, Waltham, MA), mouse α-Lz, mouse α-βgal, mouse α-
417 Notch, mouse α-Antp (Developmental Studies Hybridoma Bank, Iowa City, IA), mouse α-P1 (gift
418 from I. Ando), rabbit α-ProPO (gift from G. Christophides). Alexa Fluor 488-, Alexa Fluor 647-,
419 DyLight 405- and Cy3- conjugated secondary antibodies were used (Jackson Inmunoresearch,
420 West Grove, PA).

421 *Image acquisition and processing*

422 Lymph glands were registered in a Zeiss LSM 510 confocal microscope, either as Z-stacks or
423 single confocal planes as indicated in each case. Images were processed using ImageJ software.
424 Quantification of the area occupied by the indicated markers was performed using whole Z-
425 projections of confocal stacks or single confocal planes as mentioned in each case, and is
426 expressed as the area occupied by the marker relative to the total lobe area. In the case of CCs,
427 the total number of CCs relative to the total lobe area was quantified.

428 *Statistical analysis*

429 Two-tailed unpaired Student's t-tests or one-way ANOVAs (GraphPad Prism software) were
430 used. The threshold for statistical significance was established as $*p < 0.05$, $**p < 0.01$ or $***p$
431 < 0.001.

432

Acknowledgements

We thank U. Banerjee lab members for sharing knowledge and expertise on lymph gland work. RA. Schulz, A. Bachman and U. Banerjee for fly stocks; I. Ando and G. Christophides for the kind gift of mouse α-P1 and rabbit α-ProPO antibodies. The mouse α-Lz (U.Banerjee), mouse α-βgal (J.R. Sanes), mouse α-Notch (S. Artavanis-Tsakonas) and mouse α-Antp (D. Brower) antibodies, developed by the indicated investigators, were obtained from the Developmental Studies Hybridoma Bank, created by the NICHD of the NIH and maintained at The University of Iowa, Department of Biology, Iowa City, IA 52242. Stocks obtained from the Bloomington Drosophila Stock Center (NIH P40OD018537) and the Kyoto Stock Center were used in this study. We thank members of the Wappner lab for discussion and comments on the manuscript.

Competing interests

The authors declare no competing interests.

Funding

DBO is a fellow of Agencia Nacional de Promoción Científica y Tecnológica (ANPCyT) and was travel fellow from The Company of Biologists; MJK is a Career Investigator of Consejo Nacional de Investigaciones Científicas y Técnicas (CONICET); LD is member of FBMC (Universidad de Buenos Aires); PW is a Career Investigator of CONICET. This work was supported by ANPCyT grants PICT 2014-0649 and PICT 2015-0372 to PW.

References

1. Jung SH, Evans CJ, Uemura C, Banerjee U. The Drosophila lymph gland as a developmental model of hematopoiesis. Development. 2005;132(11):2521-33.
2. Banerjee U, Girard JR, Goins LM, Spratford CM. *Drosophila* as a Genetic Model for Hematopoiesis. Genetics. 2019;211(2):367-417.
3. Crozatier M, Vincent A. Drosophila: a model for studying genetic and molecular aspects of haematopoiesis and associated leukaemias. Dis Model Mech. 2011;4(4):439-45.
4. Evans CJ, Sinenko SA, Mandal L, Martinez-Agosto JA, Hartenstein V, Banerjee U. Genetic Dissection of Hematopoiesis Using Drosophila as a Model System. 2007;18:259-99.
5. Evans CJ, Liu T, Banerjee U. Drosophila hematopoiesis: Markers and methods for molecular genetic analysis. Methods. 2014;68(1):242-51.
6. Krzemien J, Dubois L, Makki R, Meister M, Vincent A, Crozatier M. Control of blood cell homeostasis in Drosophila larvae by the posterior signalling centre. Nature. 2007;446(7133):325-8.
7. Krzemien J, Oyallon J, Crozatier M, Vincent A. Hematopoietic progenitors and hemocyte lineages in the Drosophila lymph gland. Developmental biology. 2010;346(2):310-9.

469 8. Kurucz E, Markus R, Zsamboki J, Folkl-Medzihradszky K, Darula Z, Vilmos P, et al. Nimrod, a
470 putative phagocytosis receptor with EGF repeats in Drosophila plasmatocytes. Curr Biol. 2007;17(7):649-
471 54.
472 9. Kurucz E, Vaczi B, Markus R, Laurinyecz B, Vilmos P, Zsamboki J, et al. Definition of Drosophila
473 hemocyte subsets by cell-type specific antigens. Acta Biol Hung. 2007;58 Suppl:95-111.
474 10. Kocks C, Cho JH, Nehme N, Ulvila J, Pearson AM, Meister M, et al. Eater, a transmembrane
475 protein mediating phagocytosis of bacterial pathogens in Drosophila. Cell. 2005;123(2):335-46.
476 11. Rizki TM, Rizki RM, Grell EH. A mutant affecting the crystal cells inDrosophila melanogaster.
477 Wilehm Roux Arch Dev Biol. 1980;188(2):91-9.
478 12. Lebestky T. Specification of Drosophila Hematopoietic Lineage by Conserved Transcription
479 Factors. Science. 2000;288(5463):146-9.
480 13. Pennetier D, Oyallon J, Morin-Poulard I, Dejean S, Vincent A, Crozatier M. Size control of the
481 Drosophila hematopoietic niche by bone morphogenetic protein signaling reveals parallels with
482 mammals. Proc Natl Acad Sci U S A. 2012;109(9):3389-94.
483 14. Mandal L, Martinez-Agosto JA, Evans CJ, Hartenstein V, Banerjee U. A Hedgehog- and
484 Antennapedia-dependent niche maintains Drosophila haematopoietic precursors. Nature.
485 2007;446(7133):320-4.
486 15. Mondal BC, Mukherjee T, Mandal L, Evans CJ, Sinenko SA, Martinez-Agosto JA, et al. Interaction
487 between differentiating cell- and niche-derived signals in hematopoietic progenitor maintenance. Cell.
488 2011;147(7):1589-600.
489 16. Lebestky T, Jung SH, Banerjee U. A Serrate-expressing signaling center controls Drosophila
490 hematopoiesis. Genes Dev. 2003;17(3):348-53.
491 17. Crozatier M, Ubeda J-M, Vincent A, Meister M. Cellular Immune Response to Parasitization in
492 Drosophila Requires the EBF Orthologue Collier. PLOS Biology. 2004;2(8):e196.
493 18. Benmimoun B, Polesello C, Haenlin M, Waltzer L. The EBF transcription factor Collier directly
494 promotes Drosophila blood cell progenitor maintenance independently of the niche. Proc Natl Acad Sci
495 U S A. 2015;112(29):9052-7.
496 19. Baldeosingh R, Gao H, Wu X, Fossett N. Hedgehog signaling from the Posterior Signaling Center
497 maintains U-shaped expression and a prohemocyte population in Drosophila. Dev Biol. 2018;441(1):132-
498 45.
499 20. Bray SJ. Notch signalling in context. Nat Rev Mol Cell Biol. 2016;17(11):722-35.
500 21. Duvic B, Hoffmann JA, Meister M, Royet J. Notch Signaling Controls Lineage Specification during
501 Drosophila Larval Hematopoiesis. Current Biology.12(22):1923-7.
502 22. Mukherjee T, Kim WS, Mandal L, Banerjee U. Interaction between Notch and Hif-alpha in
503 development and survival of Drosophila blood cells. Science. 2011;332(6034):1210-3.
504 23. Ferguson GB, Martinez-Agosto JA. Yorkie and Scalloped signaling regulates Notch-dependent
505 lineage specification during Drosophila hematopoiesis. Curr Biol. 2014;24(22):2665-72.
506 24. Liu J, Sato C, Cerletti M, Wagers A. Chapter Twelve - Notch Signaling in the Regulation of Stem
507 Cell Self-Renewal and Differentiation. In: Kopan R, editor. Current Topics in Developmental Biology. 92:
508 Academic Press; 2010. p. 367-409.
509 25. Lampreia FP, Carmelo JG, Anjos-Afonso F. Notch Signaling in the Regulation of Hematopoietic
510 Stem Cell. Curr Stem Cell Rep. 2017;3(3):202-9.
511 26. Mancini SJC, Mantei N, Dumortier A, Suter U, MacDonald HR, Radtke F. Jagged1-dependent
512 Notch signaling is dispensable for hematopoietic stem cell self-renewal and differentiation. Blood.
513 2005;105(6):2340-2.
514 27. Maillard I, Koch U, Dumortier A, Shestova O, Xu L, Sai H, et al. Canonical notch signaling is
515 dispensable for the maintenance of adult hematopoietic stem cells. Cell stem cell. 2008;2(4):356-66.

516 28. Schroeder T, Just U. Notch signalling via RBP-J promotes myeloid differentiation. EMBO J.
517 2000;19(11):2558-68.
518 29. Schroeder T, Kohlhof H, Rieber N, Just U. Notch signaling induces multilineage myeloid
519 differentiation and up-regulates PU.1 expression. J Immunol. 2003;170(11):5538-48.
520 30. Kumano K, Chiba S, Shimizu K, Yamagata T, Hosoya N, Saito T, et al. Notch1 inhibits
521 differentiation of hematopoietic cells by sustaining GATA-2 expression. Blood. 2001;98(12):3283-9.
522 31. Vercauteren SM, Sutherland HJ. Constitutively active Notch4 promotes early human
523 hematopoietic progenitor cell maintenance while inhibiting differentiation and causes lymphoid
524 abnormalities in vivo. Blood. 2004;104(8):2315.
525 32. Varnum-Finney B, Xu L, Brashem-Stein C, Nourigat C, Flowers D, Bakkour S, et al. Pluripotent,
526 cytokine-dependent, hematopoietic stem cells are immortalized by constitutive Notch1 signaling. Nat
527 Med. 2000;6(11):1278-81.
528 33. Radtke F, Wilson A, Stark G, Bauer M, van Meerwijk J, MacDonald HR, et al. Deficient T cell fate
529 specification in mice with an induced inactivation of Notch1. Immunity. 1999;10(5):547-58.
530 34. Han H, Tanigaki K, Yamamoto N, Kuroda K, Yoshimoto M, Nakahata T, et al. Inducible gene
531 knockout of transcription factor recombination signal binding protein-J reveals its essential role in T
532 versus B lineage decision. Int Immunol. 2002;14(6):637-45.
533 35. Kushwah R, Guezguez B, Lee JB, Hopkins CI, Bhatia M. Pleiotropic roles of Notch signaling in
534 normal, malignant, and developmental hematopoiesis in the human. EMBO reports. 2014;15(11):1128-
535 38.
536 36. Oyallon J, Vanzo N, Krzemien J, Morin-Poulard I, Vincent A, Crozatier M. Two Independent
537 Functions of Collier/Early B Cell Factor in the Control of Drosophila Blood Cell Homeostasis. PLoS One.
538 2016;11(2):e0148978.
539 37. Tokusumi T, Shoue DA, Tokusumi Y, Stoller JR, Schulz RA. New hemocyte-specific enhancer-
540 reporter transgenes for the analysis of hematopoiesis in Drosophila. Genesis. 2009;47(11):771-4.
541 38. Dey NS, Ramesh P, Chugh M, Mandal S, Mandal L. Dpp dependent Hematopoietic stem cells give
542 rise to Hh dependent blood progenitors in larval lymph gland of Drosophila. Elife. 2016;5.
543 39. Bachmann A, Knust E. Dissection of cis-regulatory elements of the Drosophila gene Serrate.
544 Development Genes and Evolution. 1998;208(6):346-51.
545 40. Le Borgne R, Remaud S, Hamel S, Schweisguth F. Two Distinct E3 Ubiquitin Ligases Have
546 Complementary Functions in the Regulation of Delta and Serrate Signaling in Drosophila. PLOS Biology.
547 2005;3(4):e96.
548 41. Klinakis A, Lobry C, Abdel-Wahab O, Oh P, Haeno H, Buonamici S, et al. A novel tumour-
549 suppressor function for the Notch pathway in myeloid leukaemia. Nature. 2011;473(7346):230-3.
550 42. Varnum-Finney B, Purton LE, Yu M, Brashem-Stein C, Flowers D, Staats S, et al. The Notch
551 Ligand, Jagged-1, Influences the Development of Primitive Hematopoietic Precursor Cells. Blood.
552 1998;91(11):4084.
553 43. Calvi LM, Adams GB, Weibrecht KW, Weber JM, Olson DP, Knight MC, et al. Osteoblastic cells
554 regulate the haematopoietic stem cell niche. Nature. 2003;425(6960):841-6.
555 44. Fernandez L, Rodriguez S, Huang H, Chora A, Fernandes J, Mumaw C, et al. Tumor necrosis
556 factor-alpha and endothelial cells modulate Notch signaling in the bone marrow microenvironment
557 during inflammation. Exp Hematol. 2008;36(5):545-58.
558 45. Tokusumi Y, Tokusumi T, Stoller-Conrad J, Schulz RA. Serpent, suppressor of hairless and U-
559 shaped are crucial regulators of hedgehog niche expression and prohemocyte maintenance during
560 Drosophila larval hematopoiesis. Development. 2010;137(21):3561-8.
561 46. Krzemien J, Oyallon J, Crozatier M, Vincent A. Hematopoietic progenitors and hemocyte lineages
562 in the Drosophila lymph gland. Dev Biol. 2010;346(2):310-9.

563 47. Terriente-Felix A, Li J, Collins S, Mulligan A, Reekie I, Bernard F, et al. Notch cooperates with
564 Lozenge/Runx to lock haemocytes into a differentiation programme. Development. 2013;140(4):926-37.
565 48. Wilson A, MacDonald HR, Radtke F. Notch 1-deficient common lymphoid precursors adopt a B
566 cell fate in the thymus. J Exp Med. 2001;194(7):1003-12.
567 49. Pui JC, Allman D, Xu L, DeRocco S, Karnell FG, Bakkour S, et al. Notch1 expression in early
568 lymphopoiesis influences B versus T lineage determination. Immunity. 1999;11(3):299-308.
569 50. Evans CJ, Olson JM, Ngo KT, Kim E, Lee NE, Kuoy E, et al. G-TRACE: rapid Gal4-based cell lineage
570 analysis in Drosophila. Nat Methods. 2009;6(8):603-5.

571

Figure 1

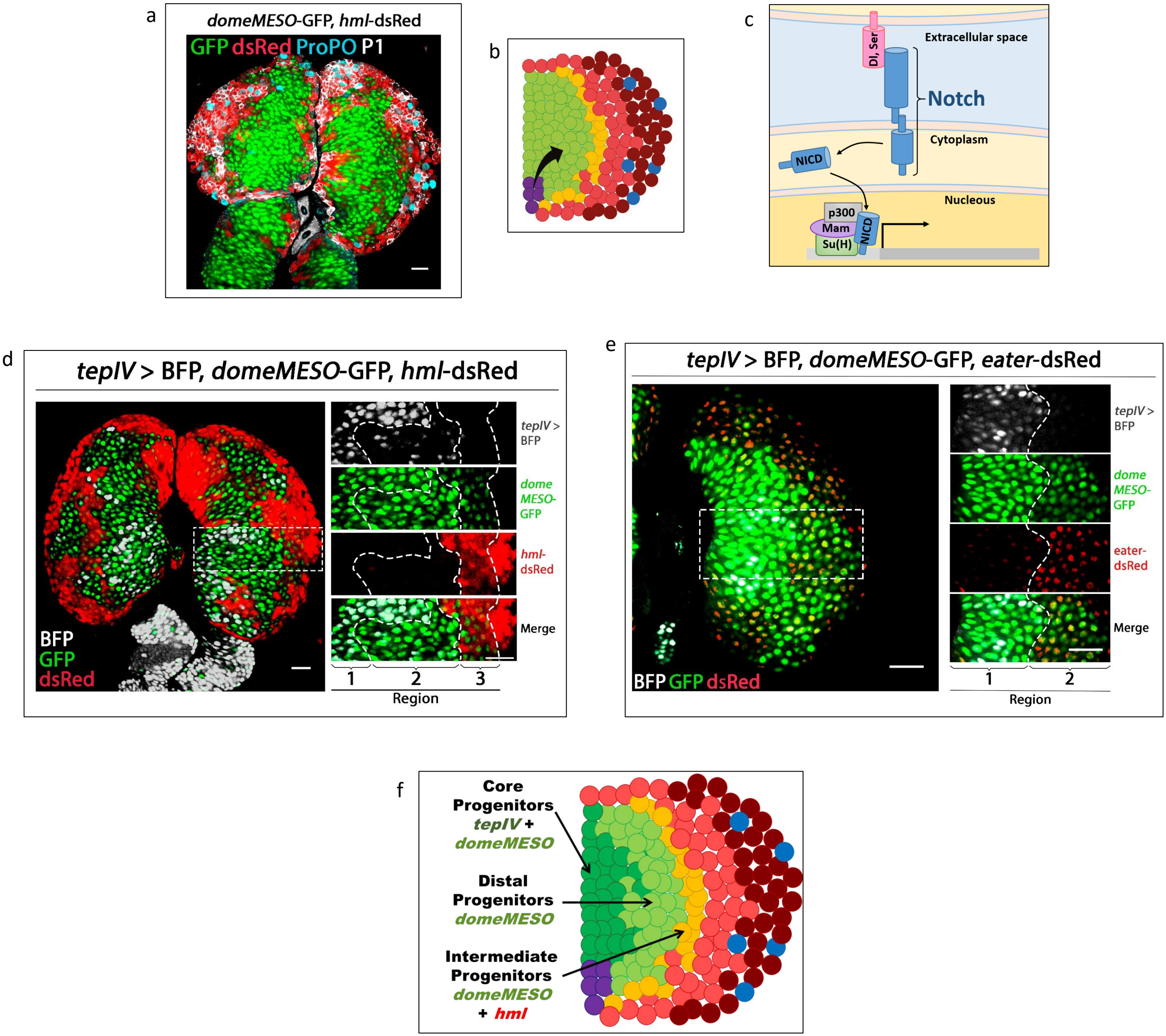
a
domeMESO-GFP, hml-dsRed
GFP dsRed ProPO P1
b
c
Dl, Ser
Extracellular space
Notch
Cytoplasm
NICD
Nucleous
p300
Mam
Su(H)
NICD
d
tepIV > BFP, domeMESO-GFP, hml-dsRed
BFP
GFP
dsRed
tepIV > BFP
dome MESO-GFP
hml-dsRed
Merge
1
2
3
Region
e
tepIV > BFP, domeMESO-GFP, eater-dsRed
BFP GFP dsRed
tepIV > BFP
dome MESO-GFP
eater-dsRed
Merge
1
2
Region
f
Core Progenitors
tepIV +
domeMESO
Distal Progenitors
domeMESO
Intermediate Progenitors
domeMESO
+ hml

Figure 2

a

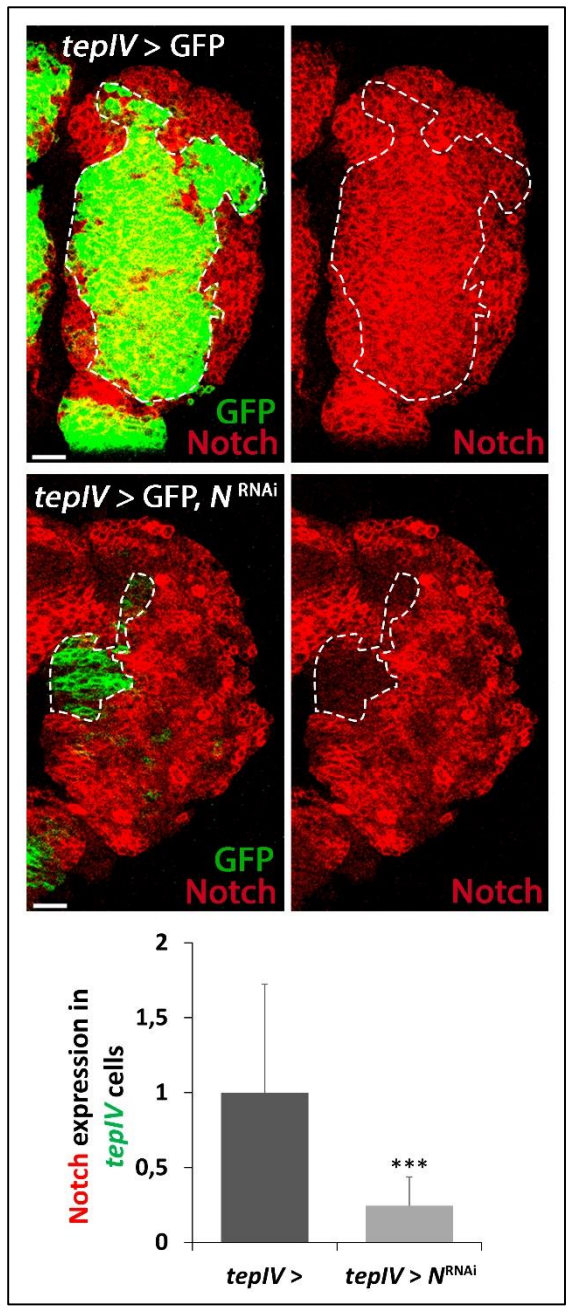

b

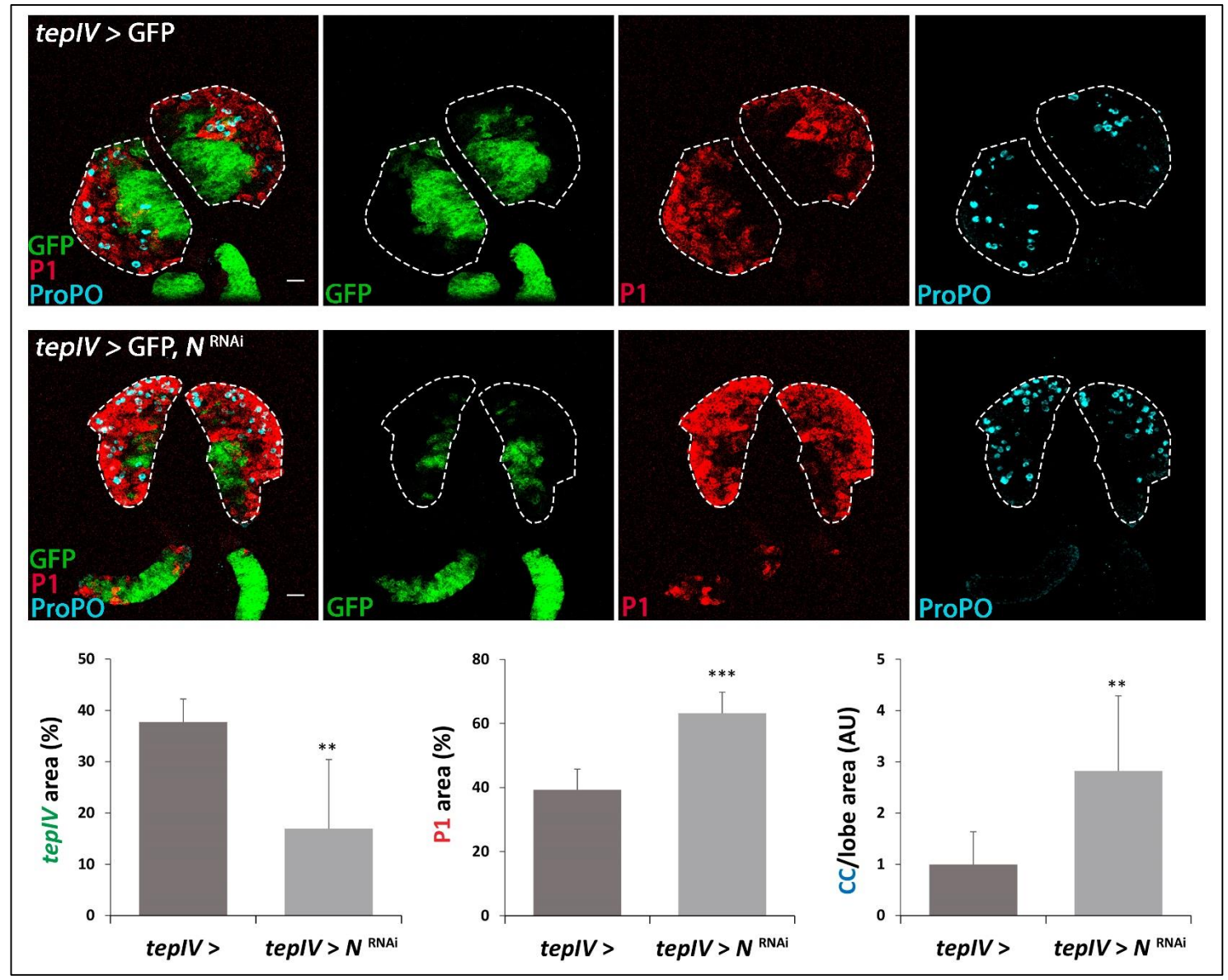

c

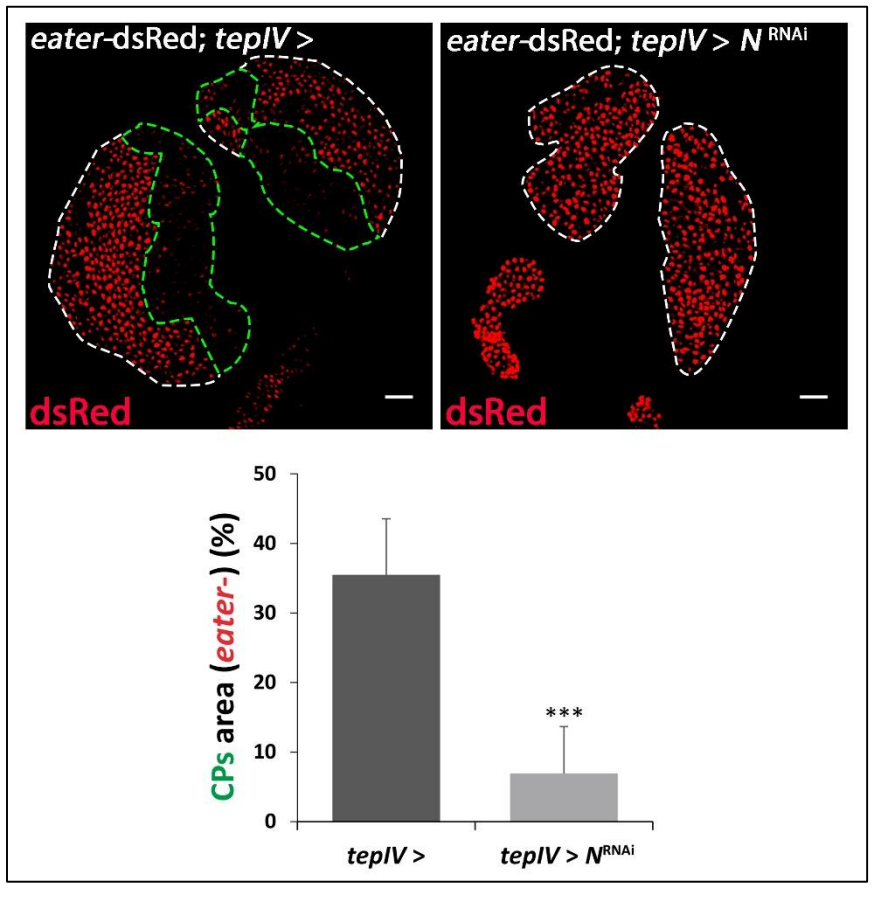

d

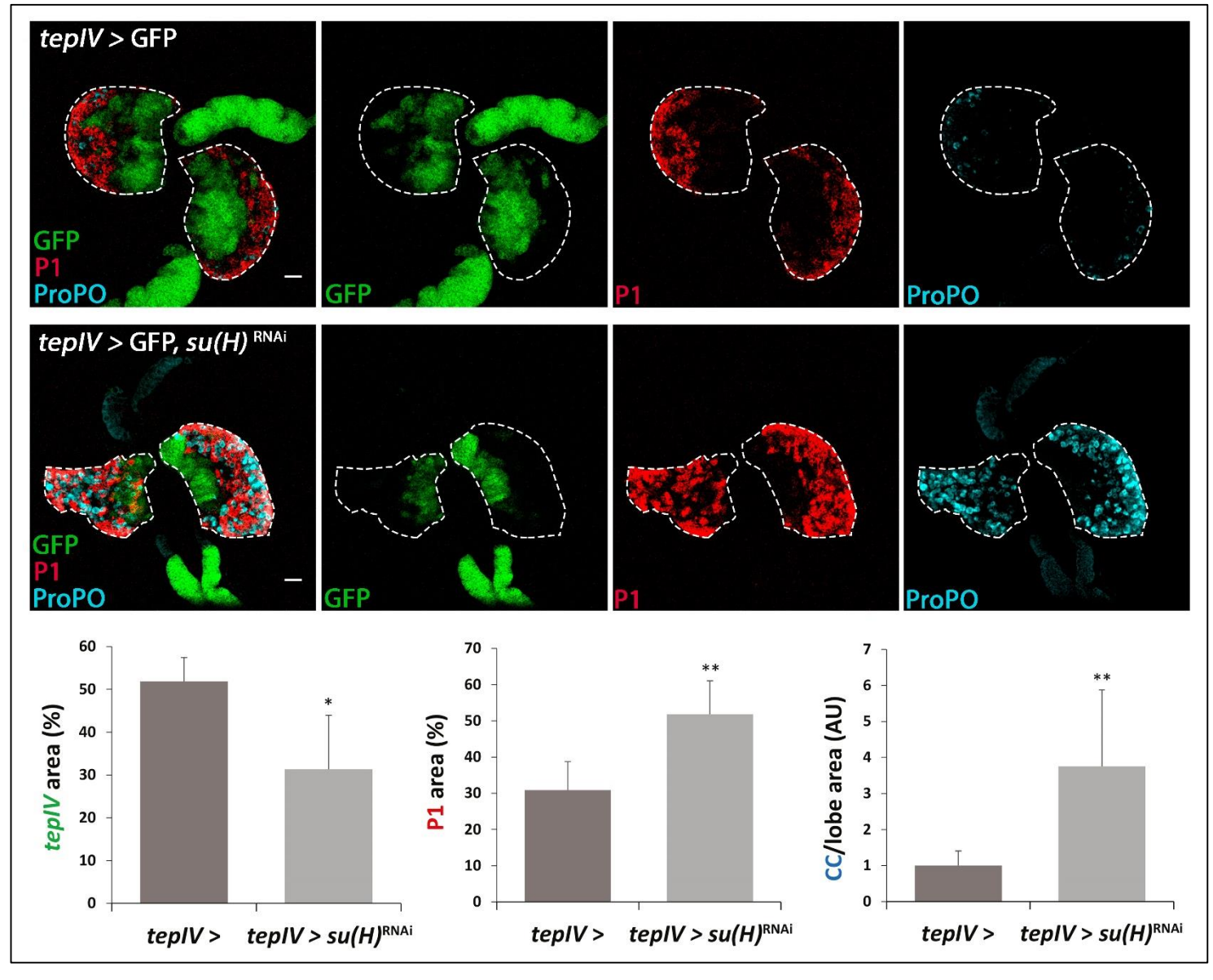

Figure 3

a

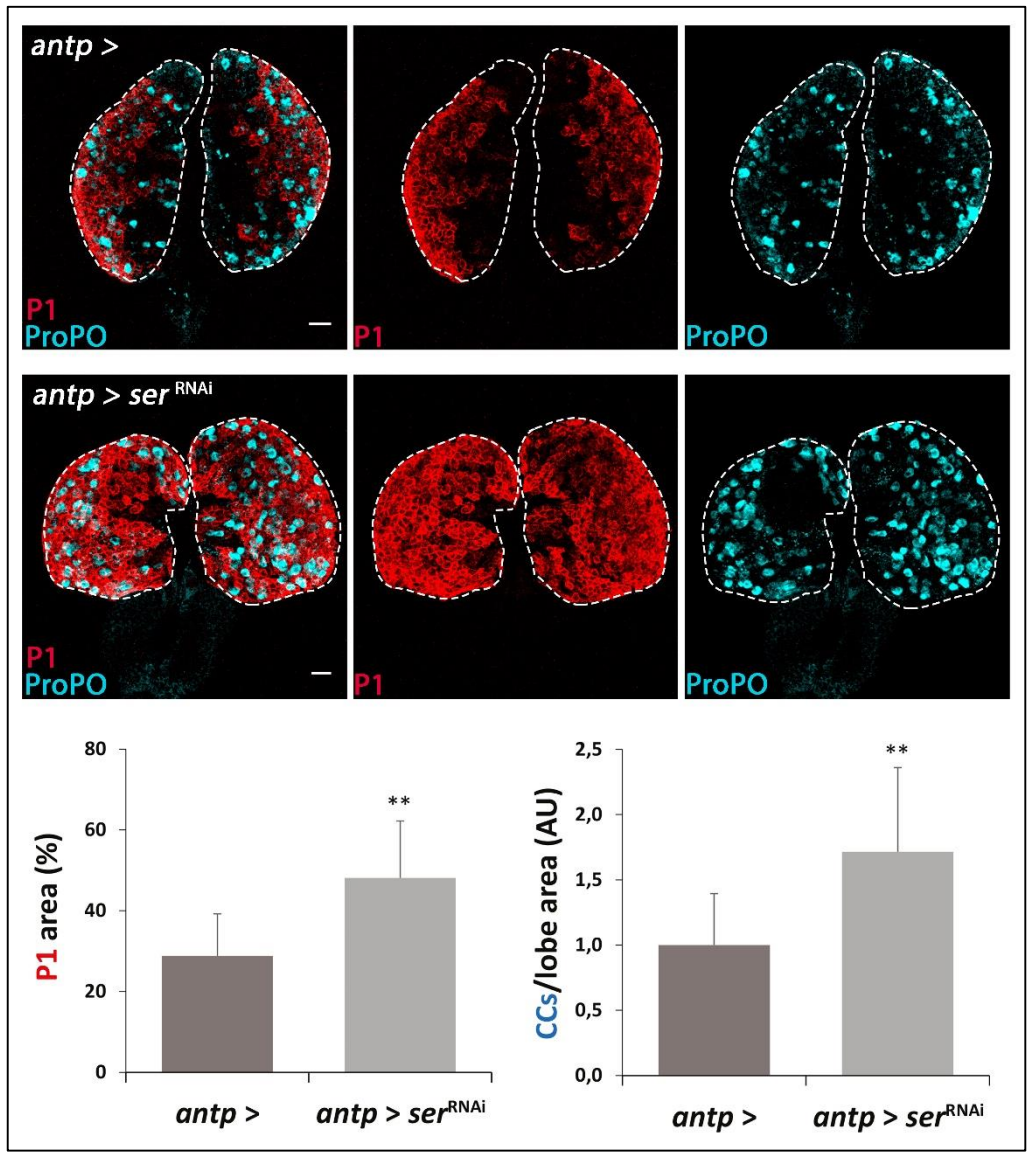

b

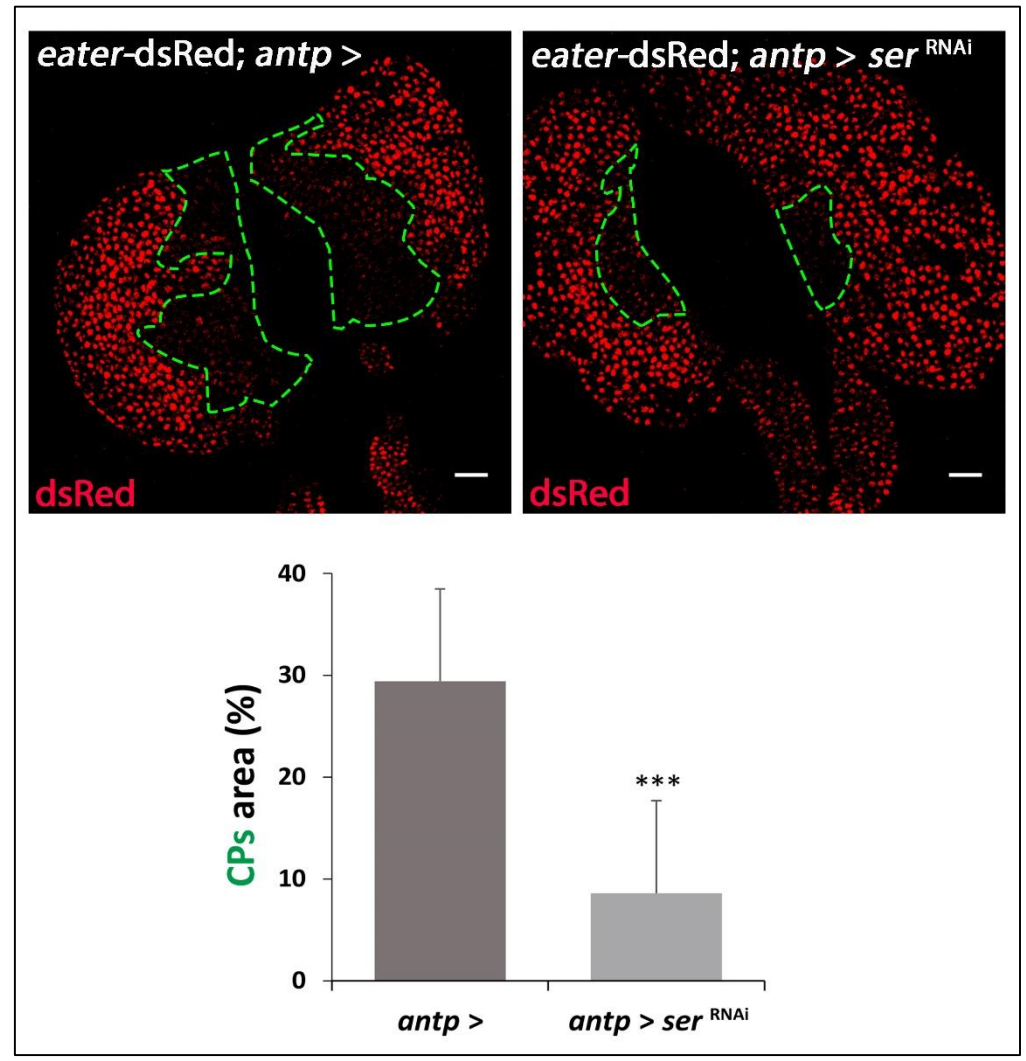

c

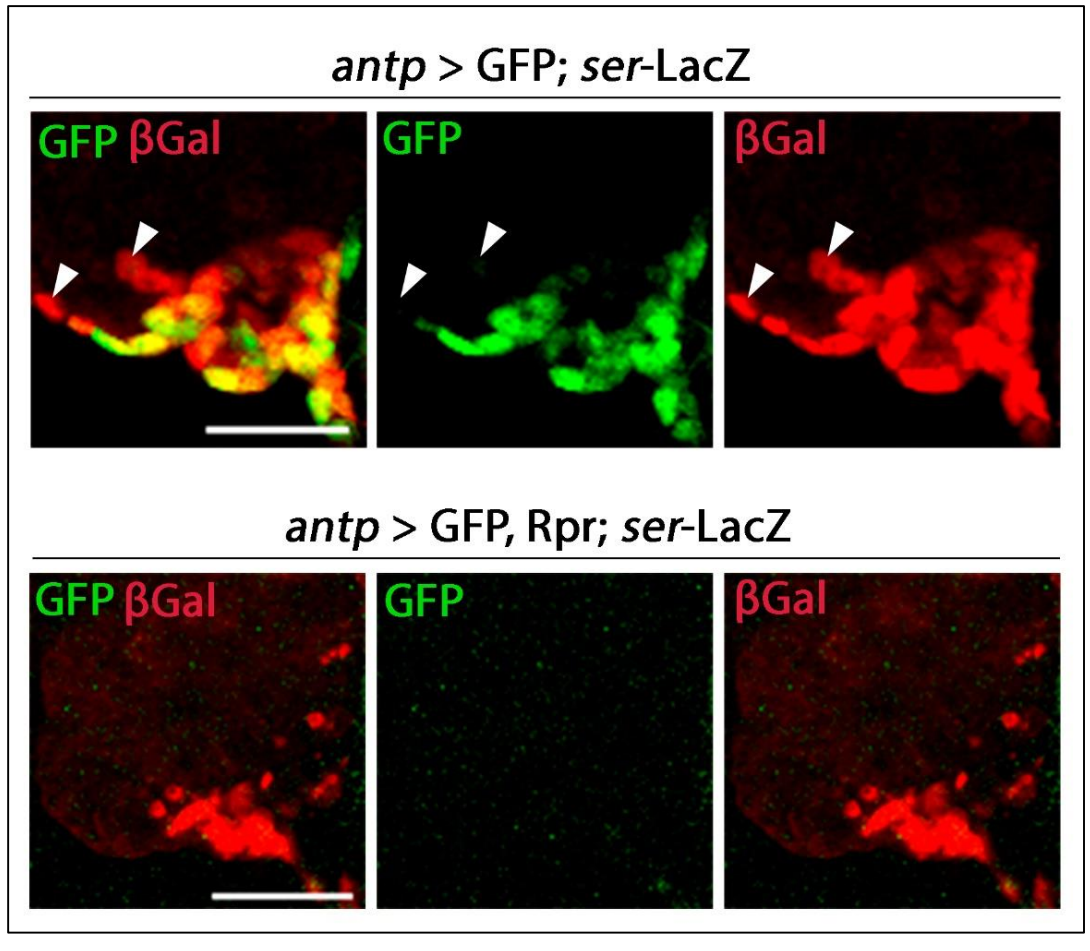

d

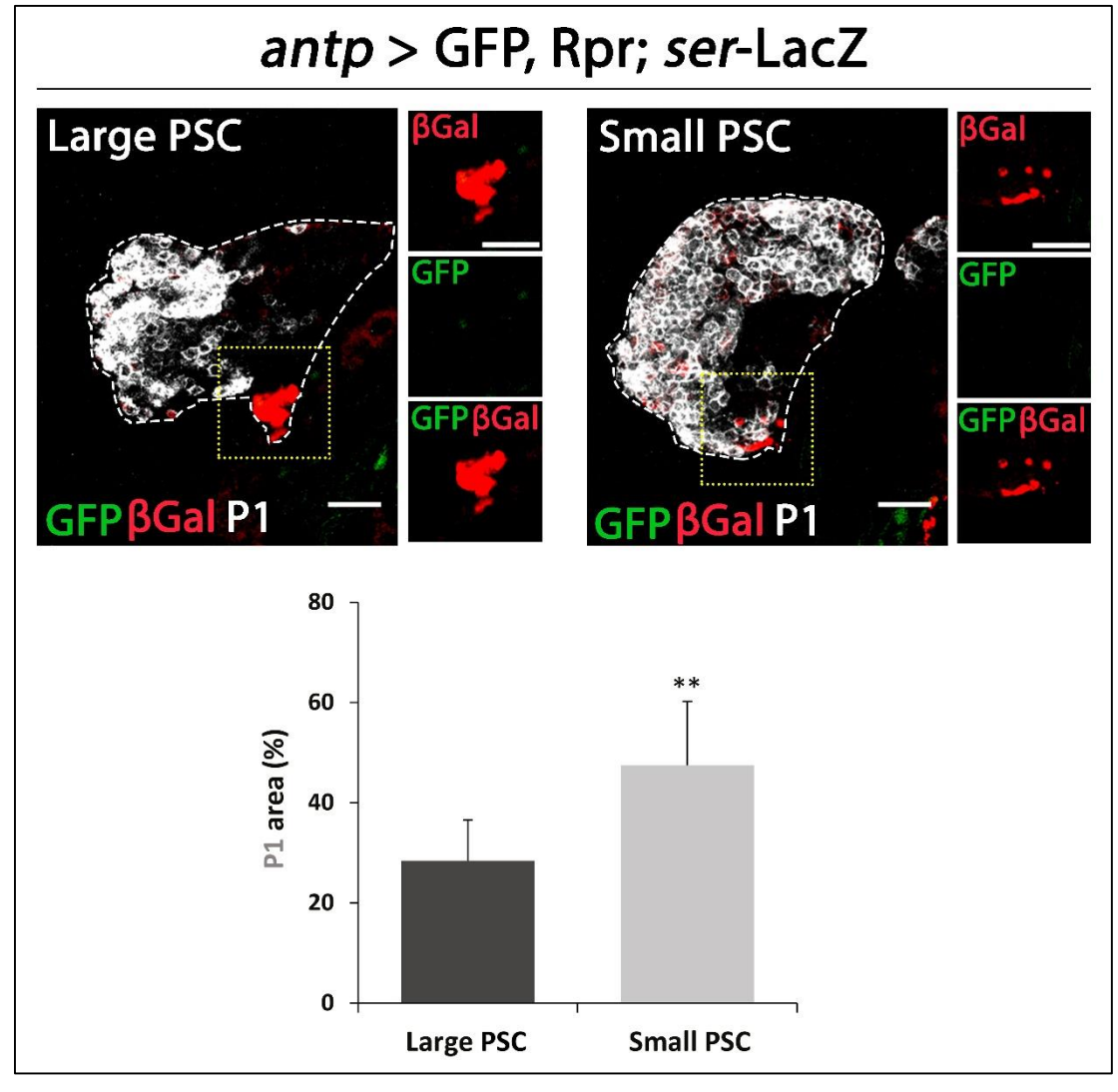

Figure 4

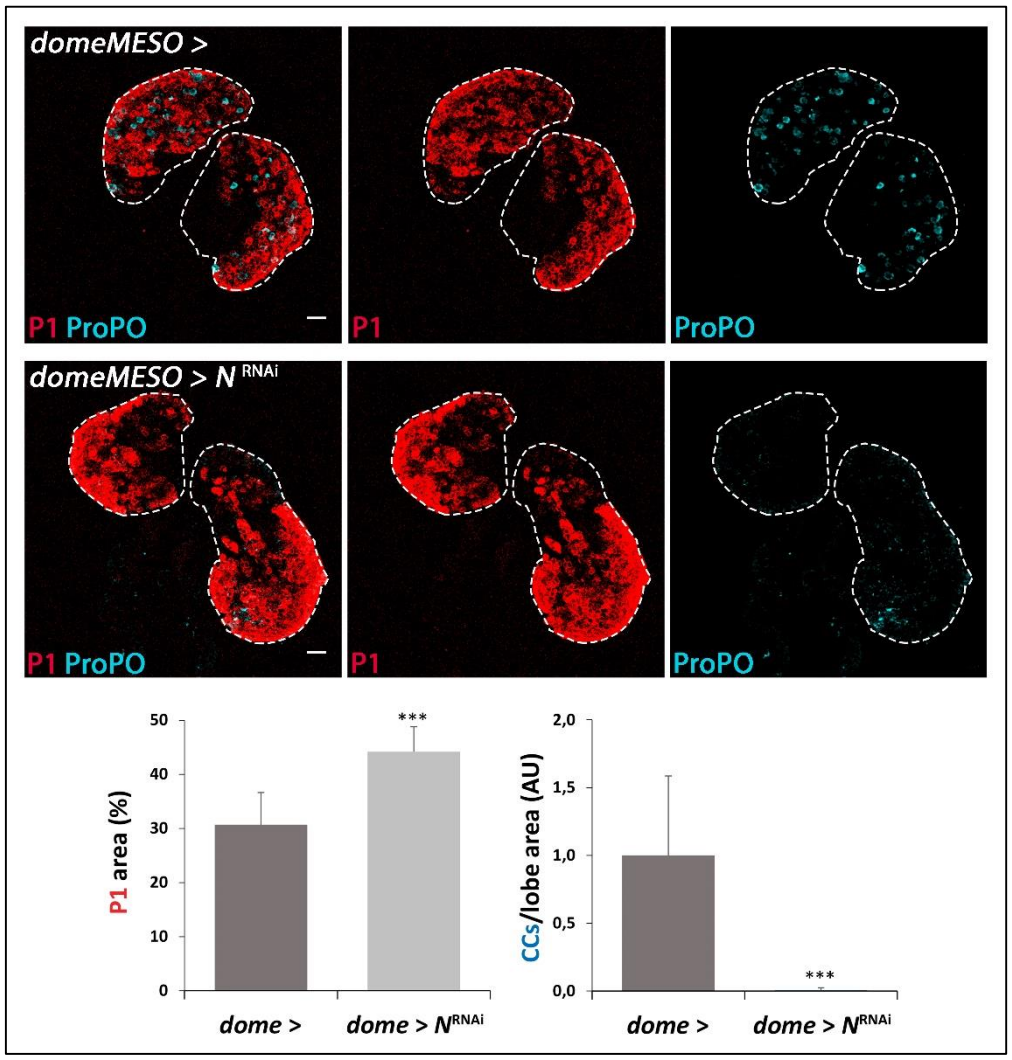
a
domeMESO >
P1 ProPO
P1
ProPO
domeMESO > N RNAi
P1 ProPO
P1
ProPO
P1 area (%)
***
CCs/lobe area (AU)
***
dome >
dome > N RNAi
dome >
dome > N RNAi

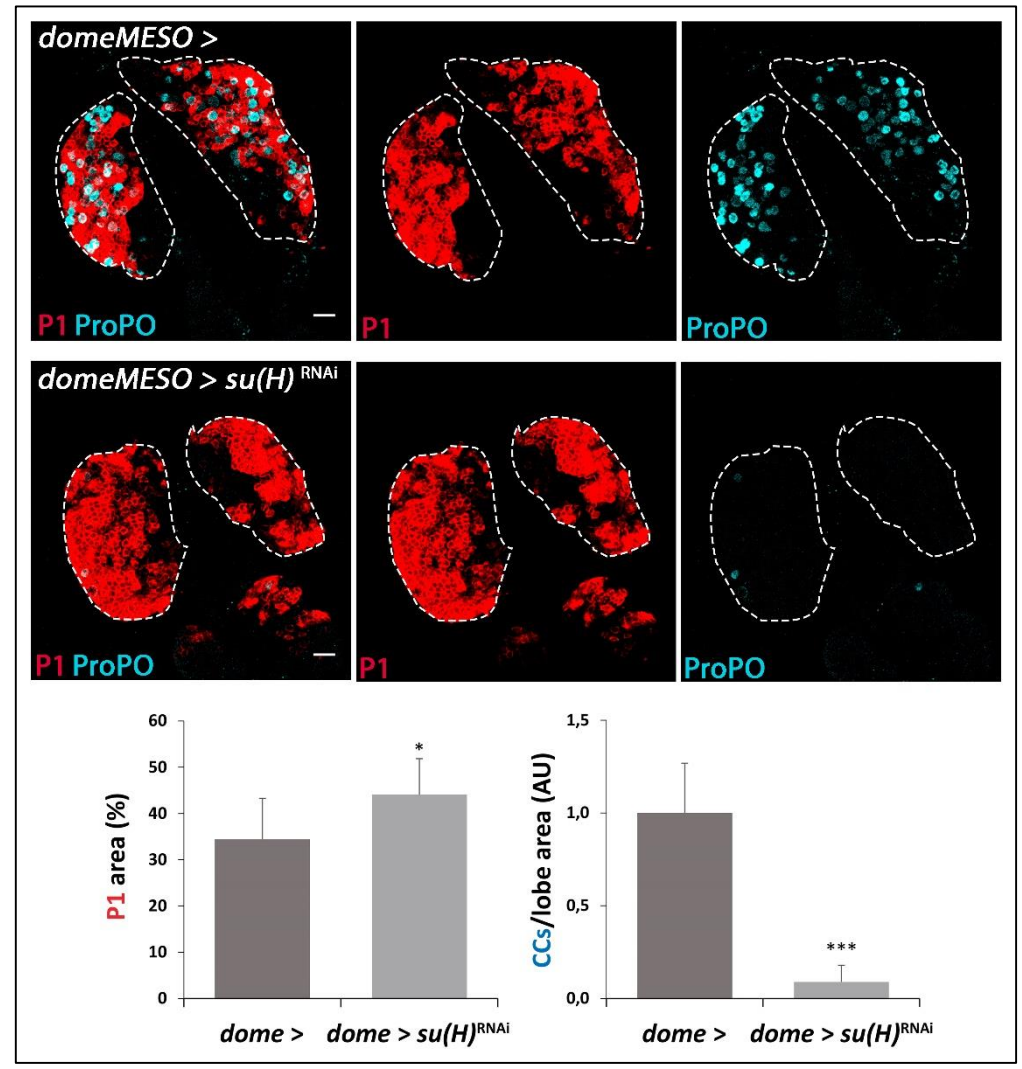
b
domeMESO >
P1 ProPO
P1
ProPO
domeMESO > su(H) RNAi
P1 ProPO
P1
ProPO
P1 area (%)
*
CCs/lobe area (AU)
***
dome >
dome > su(H) RNAi
dome >
dome > su(H) RNAi

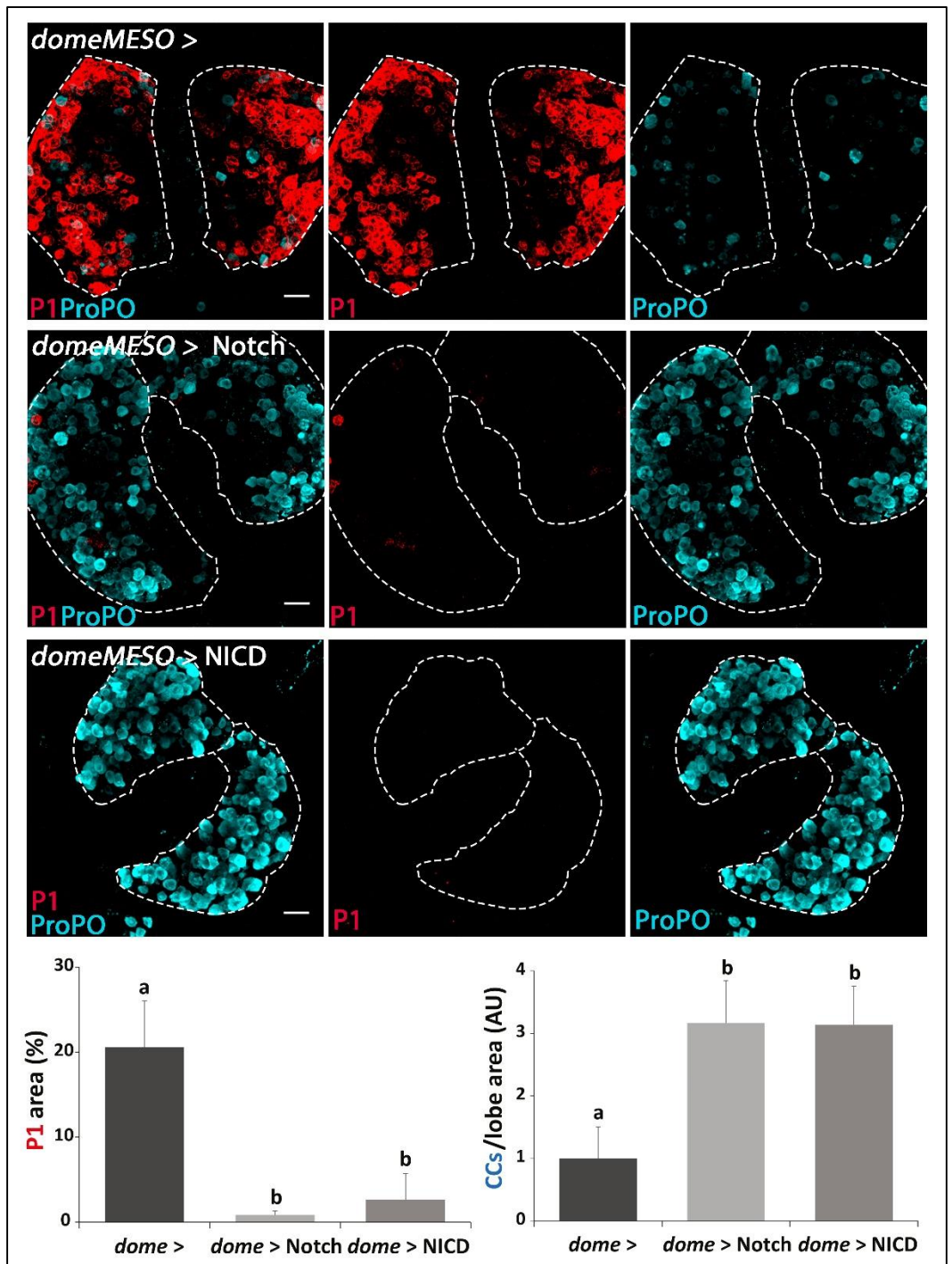
c
domeMESO >
P1ProPO
P1
ProPO
domeMESO > Notch
P1ProPO
P1
ProPO
domeMESO > NICD
P1
ProPO
P1
ProPO
P1 area (%)
a
b
b
CCs /lobe area (AU)
a
b
b
dome >
dome > Notch
dome > NICD
dome >
dome > Notch
dome > NICD

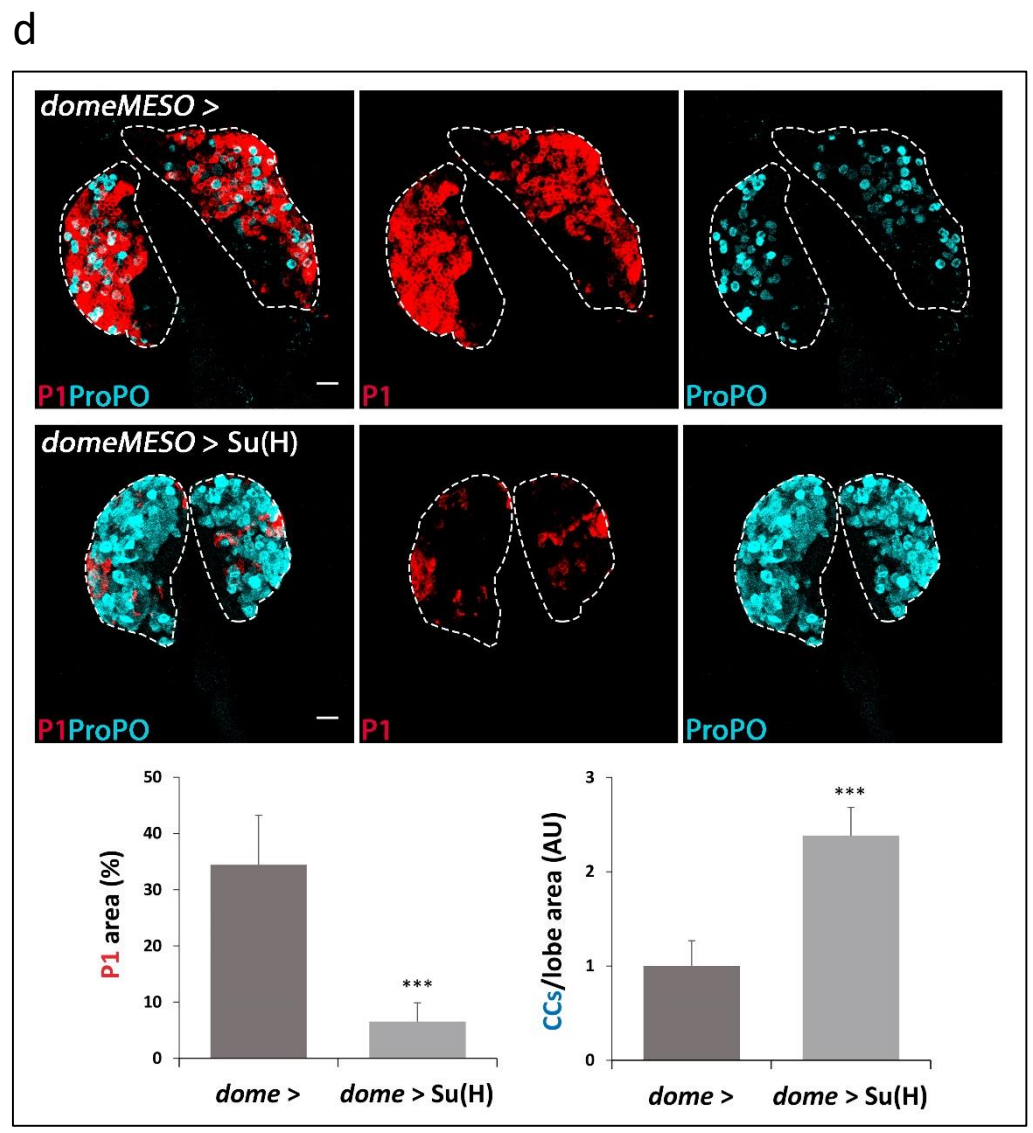
d
domeMESO >
P1ProPO
P1
ProPO
domeMESO > Su(H)
P1ProPO
P1
ProPO
P1 area (%)
***
CCs/lobe area (AU)
***
dome >
dome > Su(H)
dome >
dome > Su(H)

Figure 5

a

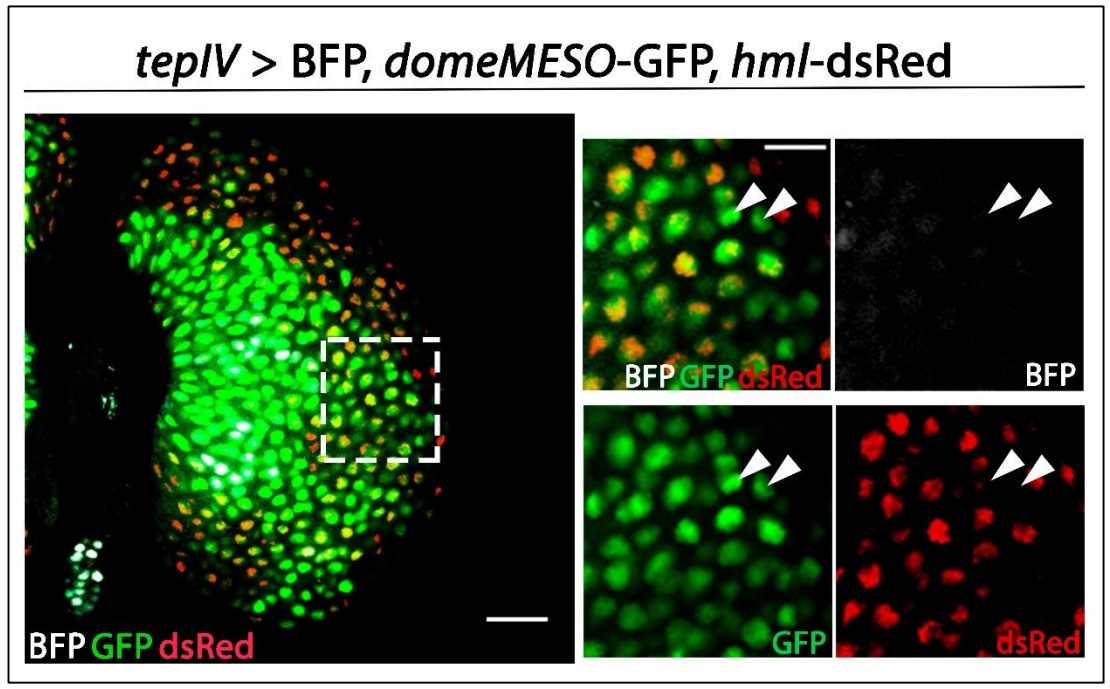

b

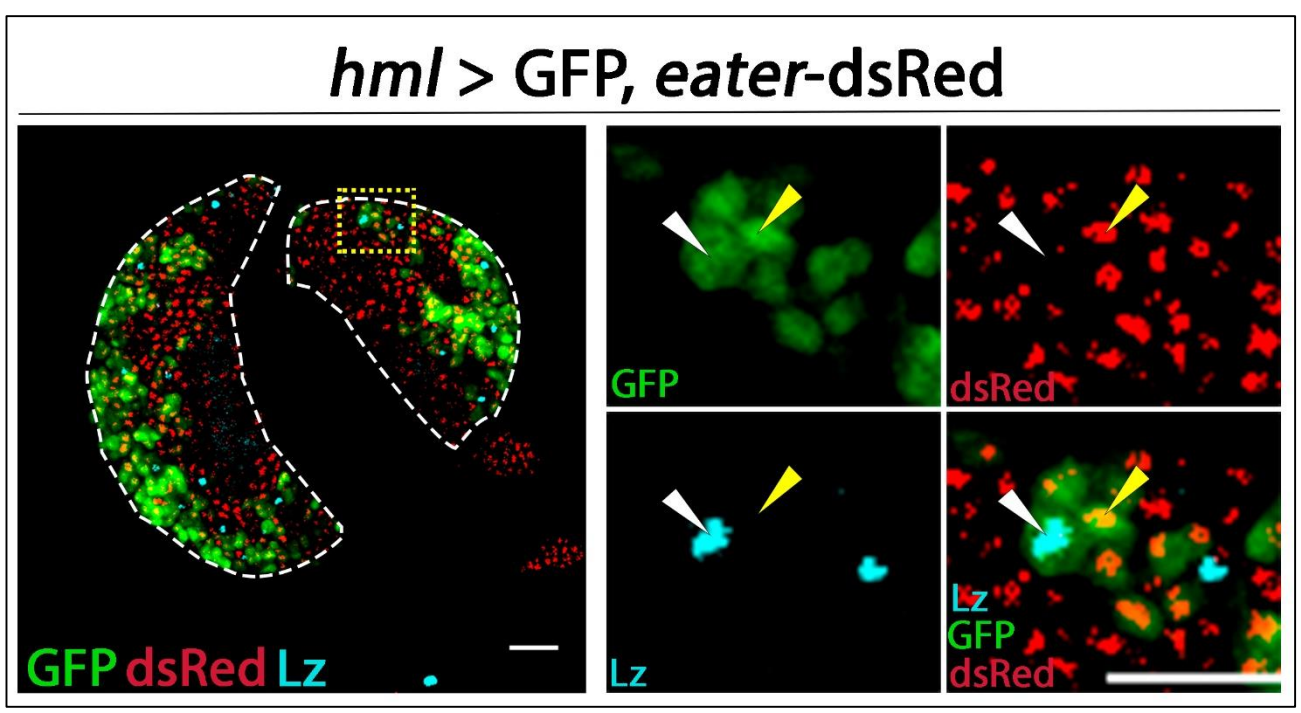

d

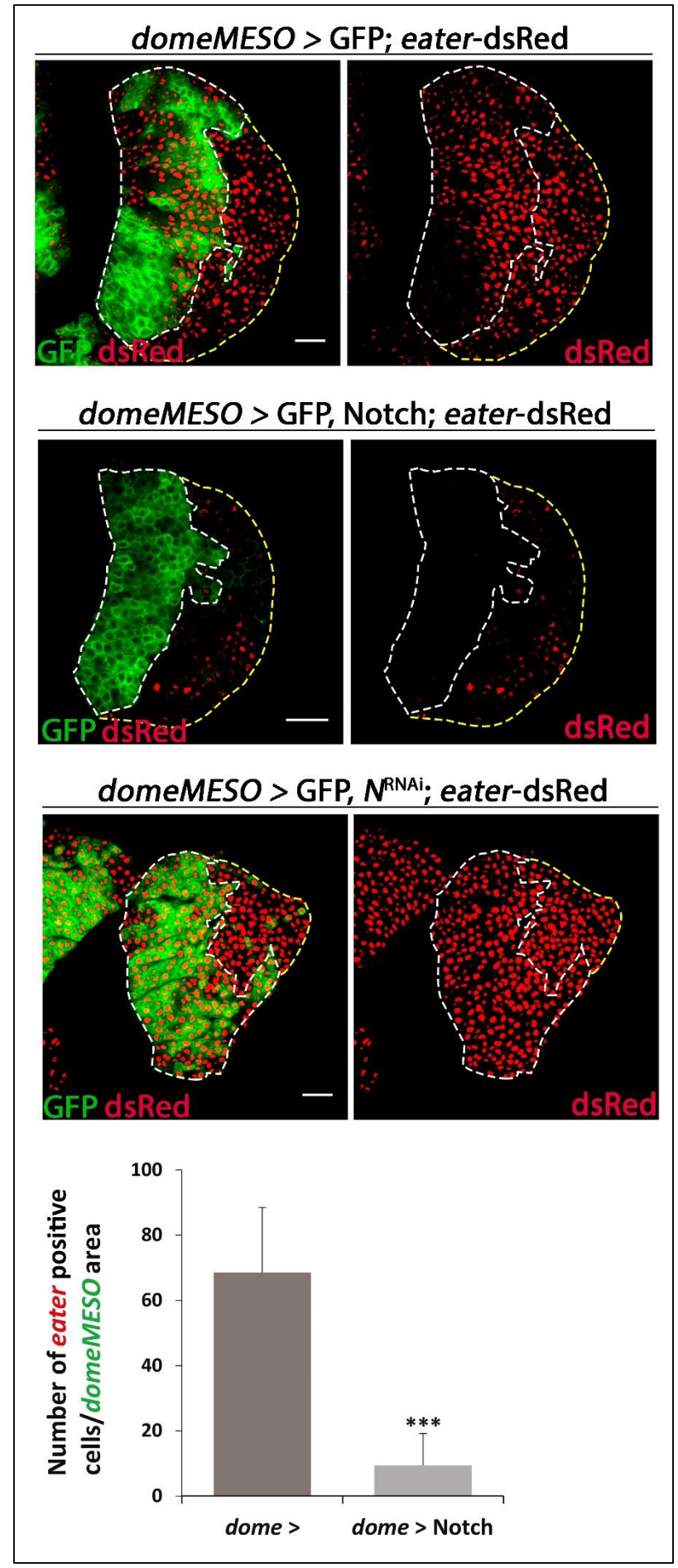

c

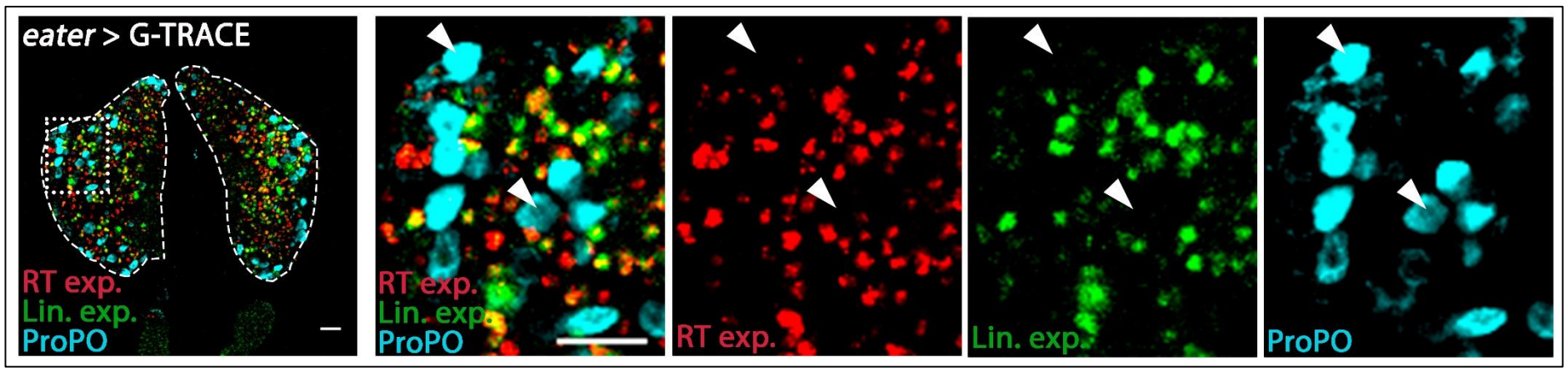

Figure 6

a

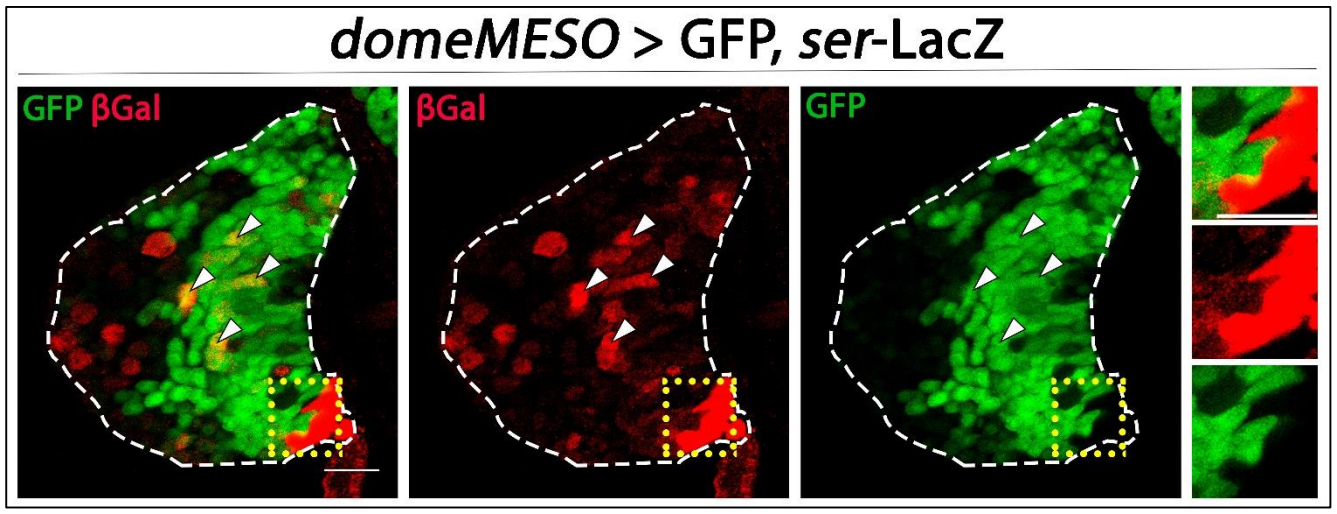

b

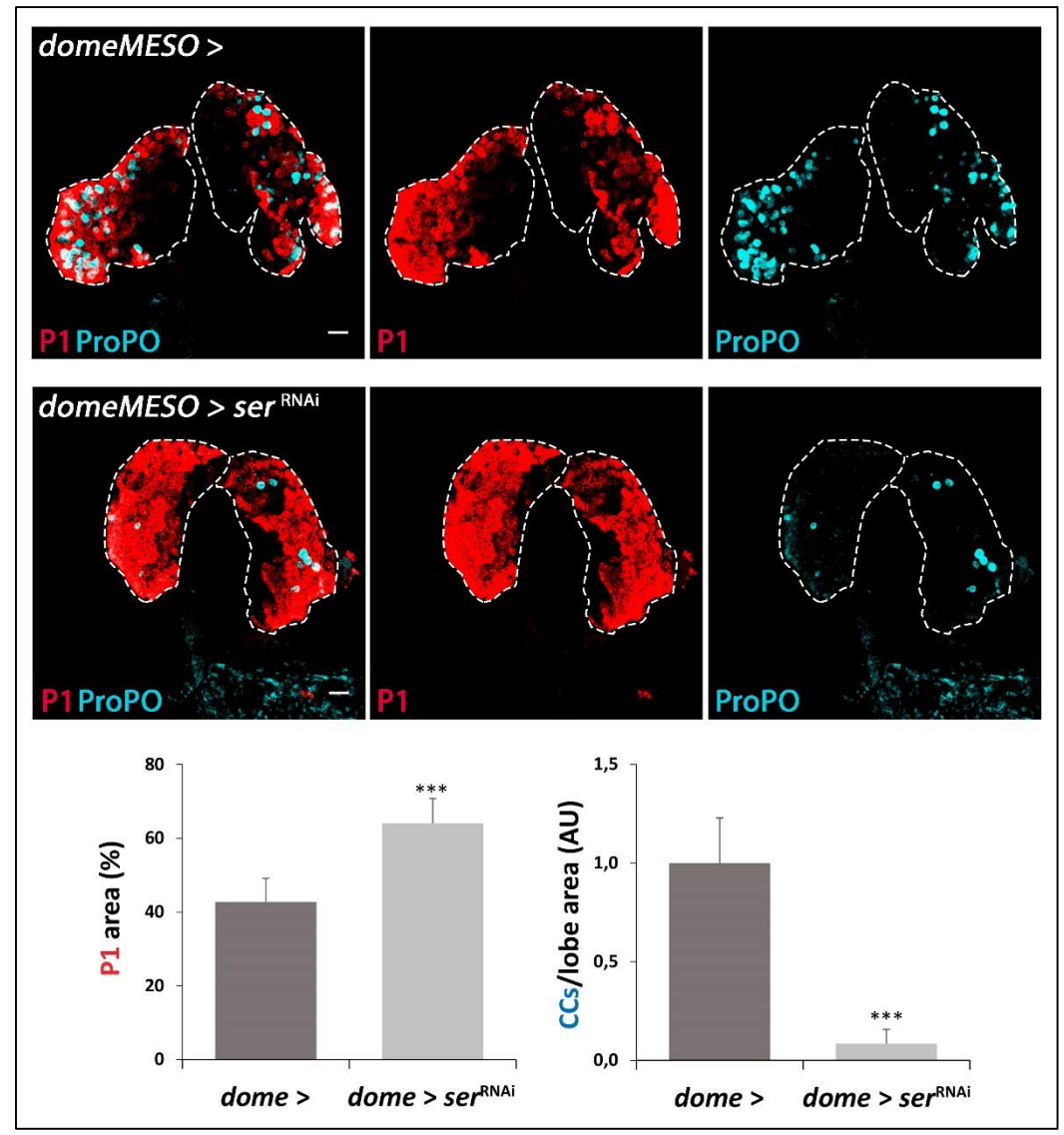

c

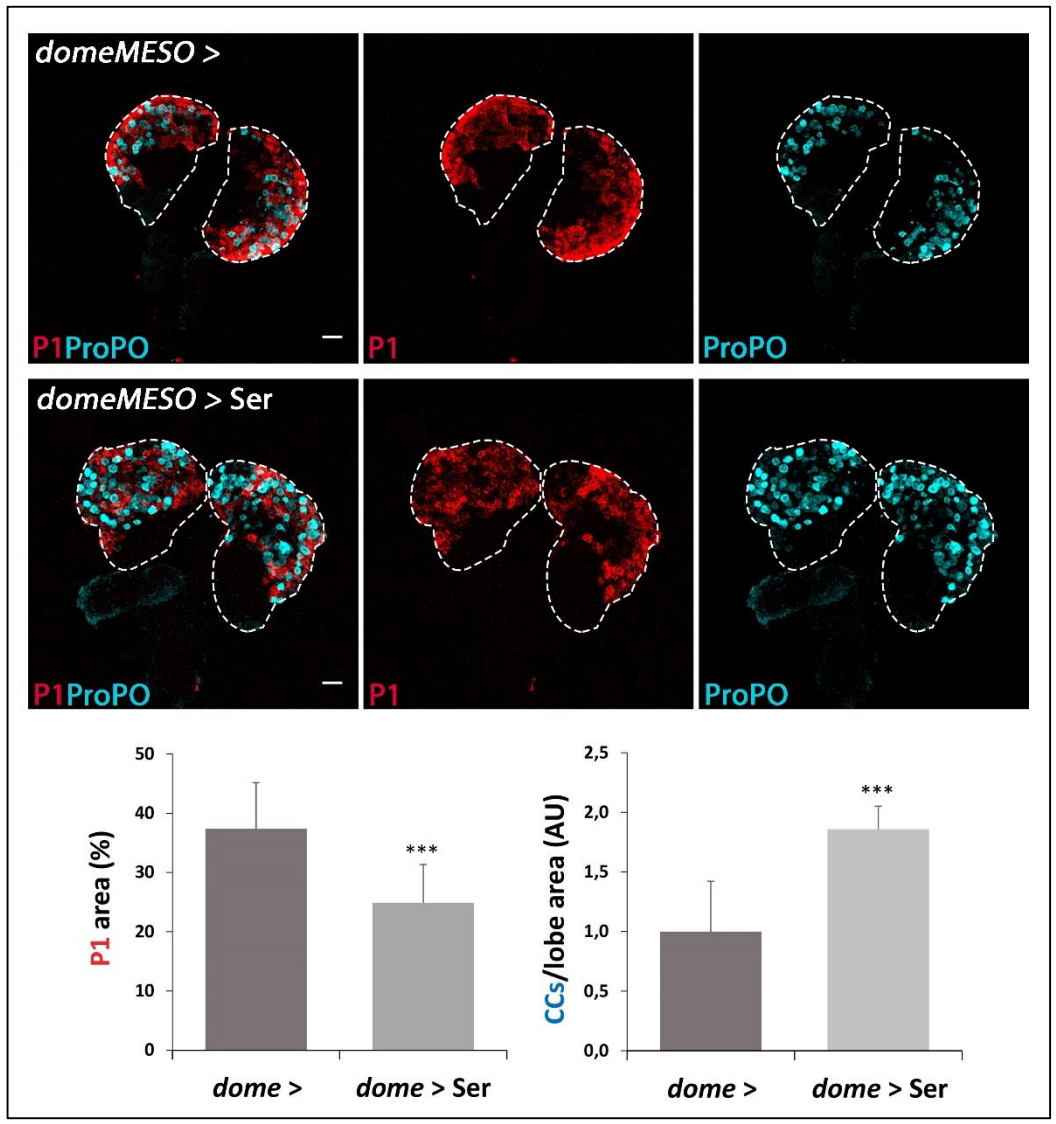

d

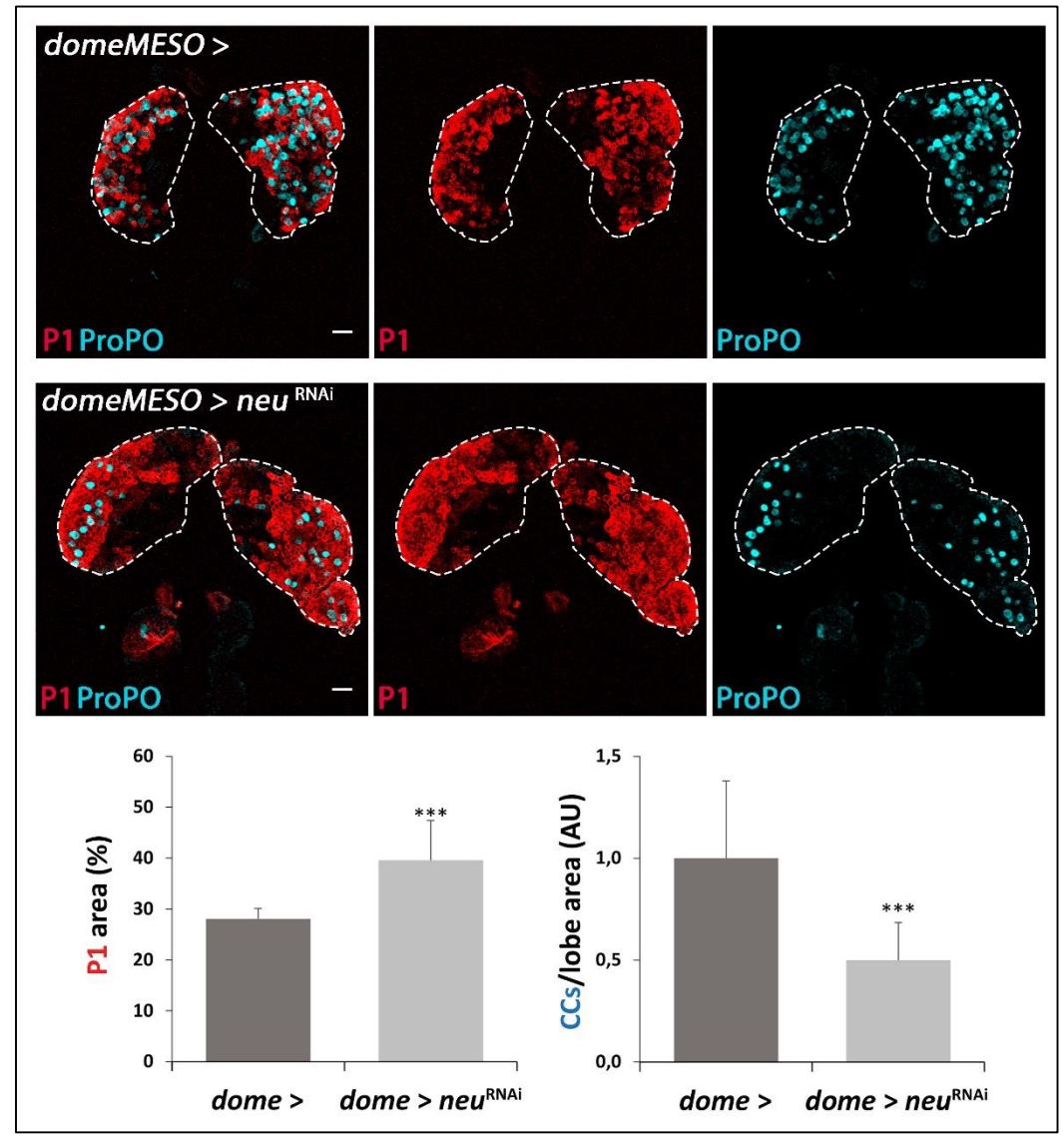

Figure 7

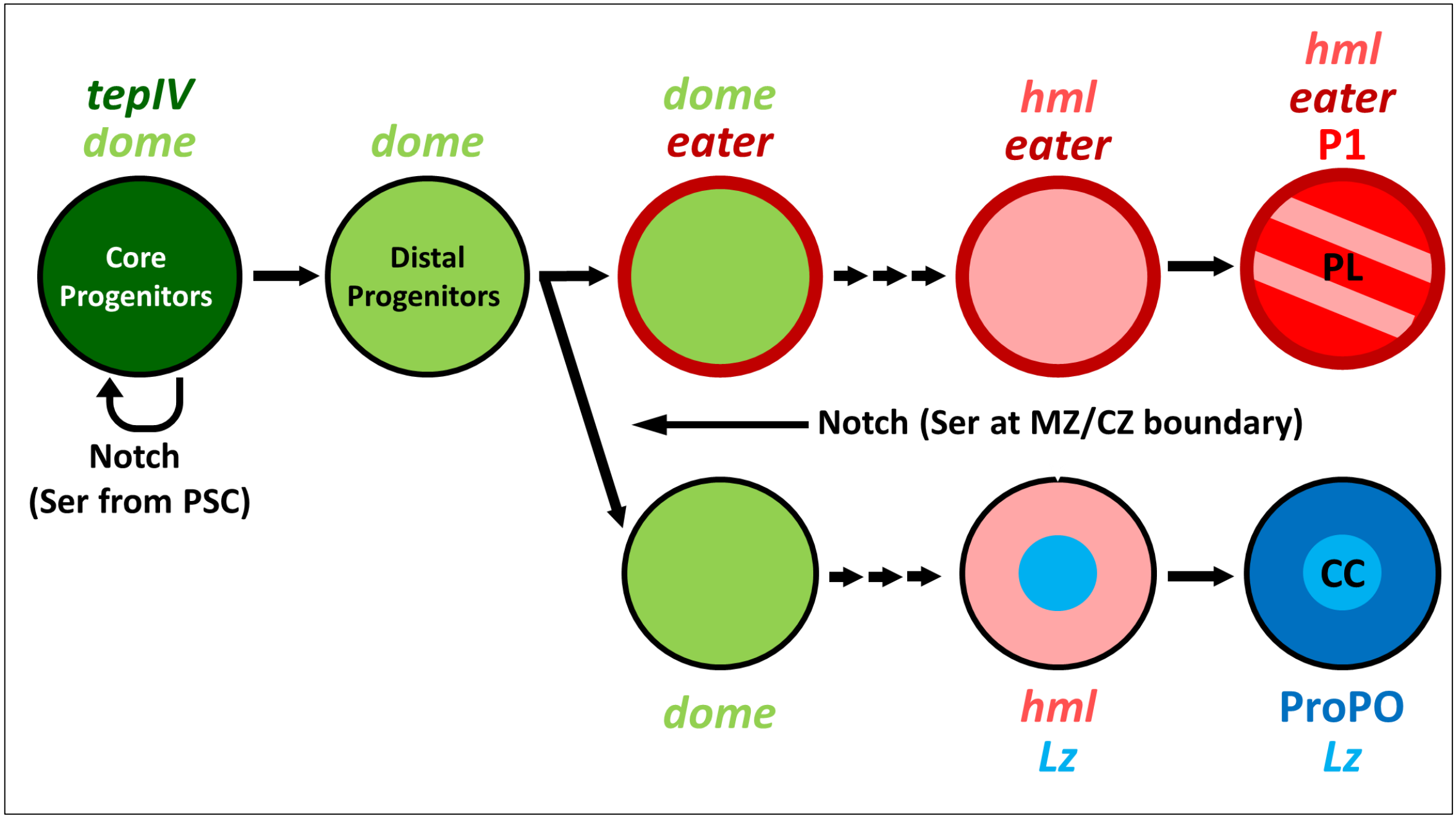
tepIV
dome
Core
Progenitors
Notch
(Ser from PSC)
dome
Distal
Progenitors
dome
eater
hml
eater
hml
eater
P1
PL
Notch (Ser at MZ/CZ boundary)
dome
hml
Lz
CC
ProPO
Lz

570 # Figure legends
571
572 **Figure 1. Progenitor populations of the lymph gland**
573 **(a) Cell populations of the lymph gland.** Blood cell progenitors (green; *domeMESO*-GFP);
574 differentiating cells (red; *hml*-dsRed); Crystal Cells (cyan, anti-ProPO staining) and
575 Plasmatocytes (white, anti-P1 staining). Single-plane confocal images of primary lobes from
576 wandering third instar larvae are shown. Scale bar, 20 µm.
577 **(b) Schematic representation of a wandering 3rd instar lymph gland lobe.** Purple: Posterior
578 Signaling Center; green: Blood cell progenitors; yellow: Intermediate Progenitors; pink:
579 Differentiating cells; dark red: Plasmatocytes; blue: Crystal Cells. The black arrow indicates
580 progenitor maintenance signals that emanate from the PSC.
581 **(c) Simplified scheme of the Notch pathway.** Dl: Delta, Ser: Serrate. NICD: Notch Intracellular
582 Domain, Su(H): Supressor of Hairless, Mam: Mastermind.
583 **(d) Three populations of blood cell progenitors occur in the lymph gland.** Region 1: Cells that
584 express both *tepIV* > BFP (white) and *domeMESO*-GFP (green). Region 2: Cells that express
585 *domeMESO*-GFP but not *tepIV* > BFP or *hml*-dsRed (red). Region 3: Cells in which *domeMESO*-
586 GFP and *hml*-dsRed signals coexist. Single-plane confocal images of primary lobes from
587 wandering third instar larvae are shown. Scale bar, 20 µm.
588 **(e) The Plasmatocyte marker *eater* is expressed in a subpopulation of blood cell progenitors.**
589 Progenitors that express both *tepIV* > BFP (white) and *domeMESO*-GFP (green) co-express
590 almost undetectable levels of the plasmatocyte marker *eater*-dsRed (red) (region 1). In
591 contrast, *eater*-dsRed expression can be readily detected in Distal Progenitors that are
592 *domeMESO*-GFP positive and negative for *tepIV* > BFP (region 2). Single-plane confocal images
593 of primary lobes from wandering third instar larvae are shown. Scale bar, 20 µm.
594 **(f) Schematic representation of a wandering 3rd instar wild-type lymph gland lobe with**
595 **redefined progenitor populations.** Progenitors encompass three subpopulations: 1) Core
596 Progenitors, positive for *domeMESO* and *tepIV* (dark green); 2) Distal Progenitors, negative for
597 *tepIV* and *hml* and positive for *domeMESO* (light green); and 3) Intermediate Progenitors,
598 which are positive for both *domeMESO* and *hml* (yellow). The color code for the remaining cell
599 populations are as in Fig. 1b: Purple: Posterior Signaling Center; pink: *hml*-positive
600 differentiating cells; dark red: Plasmatocytes; blue: Crystal Cells.
601
602
603 **Figure 2. The Notch pathway is required for Core Progenitor maintenance.**
604 **(a) Notch is expressed throughout the lymph gland.** Staining with an anti-Notch antibody
605 (red) in control lymph glands (upper panels), or in lymph glands expressing a *tepIV*-Gal4 driven
606 *notch* RNAi (N^{RNAi}) (middle panels). Single-plane confocal images of primary lobes from
607 wandering third instar larvae are shown. Scale bars, 20 µm. *TepIV* > GFP marks the area of Core
608 Progenitors, which is also delimited with a white dashed line. Note that following N^{RNAi}
609 expression, Notch staining was reduced in CPs (middle panels). Lower panel: Quantification of
610 mean anti-Notch signal levels in Core Progenitors (***$p < 0.001$). Error bars represent SD.
611 *tepIV* >, n = 16; *tepIV* > N^{RNAi}, n = 18.
612 **(b) Notch is required for Core Progenitor maintenance.** *Notch* RNAi (N^{RNAi}) expression in Core
613 Progenitors, driven by *tepIV*-Gal4, provoked loss of Core Progenitors (green: *tepIV* > GFP),
614 along with increased Plasmatocytes (red: P1 staining) and Crystal Cells (cyan: ProPO staining).
615 Compare control lymph glands in upper panels with lymph glands expressing N^{RNAi} in middle
616 panels. Whole Z-projection confocal images of primary lobes from wandering third instar

larvae are depicted. Graphs in lower panels show quantification of the indicated markers (**p < 0.01, ***p < 0.001). Error bars represent SD. *tepIV* >, n = 8; *tepIV* > N^{RNAi}, n = 8.

(c) *eater*-dsRed reporter expression domain is expanded upon Core Progenitor loss. Expression of the *eater*-dsRed reporter (red) in control lymph glands (left panel) and in lymph glands expressing *notch* RNAi (N^{RNAi}) in Core Progenitors under the *tepIV*-Gal4 driver (right panel). The green dashed line marks *eater*-negative Core Progenitors area. Single-plane confocal images of primary lobes from wandering third instar larvae are shown. The graph shows quantification of *eater*-negative area corresponding to Core Progenitors (***p < 0.001). Error bars represent SD. *tepIV* > , n = 8; *tepIV* > N^{RNAi}, n = 15.

(d) Supressor of Hairless (Su(H)) is required for Core Progenitor maintenance. $Su(H)^{RNAi}$ expression with *tepIV*-Gal4 caused a reduction of Core Progenitors (green: *tepIV* > GFP), and a simultaneous increase of Plasmatocytes (red: P1 staining) and Crystal Cells (cyan: ProPO staining). Upper panels: Controls without RNAi; Middle panels: Expression of $su(H)^{RNAi}$. Whole Z-projection confocal images of primary lobes from wandering third instar larvae are depicted. Graphs in lower panels show quantification of the indicated markers (*p < 0.05, **p < 0.01). Error bars represent SD. *tepIV* >, n = 8; *tepIV* > $su(H)^{RNAi}$, n = 5.

Figure 3. Serrate is required at the Posterior Signaling Center for Core Progenitor maintenance.

(a) *Serrate (Ser)* silencing at the Posterior Signaling Center provokes increased differentiation of Plasmatocytes and Crystal Cells. Following *serrate* RNAi (ser^{RNAi}) expression with an *antp*-Gal4 driver, a general increase of cell differentiation was observed. Plasmatocytes are in red (P1 staining) and Crystal Cells in cyan (ProPO staining). Upper panels: Control lymph glands; middle panels: Lymph glands with expression of ser^{RNAi} driven by *antp*-Gal4. Whole Z-projection confocal images of primary lobes from wandering third instar larvae are shown. Scale bars, 20 µm. Lower panels: Quantification of the results (**p < 0.01). Error bars represent SD. *Antp* >, n = 10; *antp* > ser^{RNAi}, n = 14.

(b) *Serrate* (*ser*) silencing at the Posterior Signaling Center provokes a reduction of Core Progenitors. Expression of the *eater*-dsRed reporter is shown, and the area that lacks its expression corresponds to Core Progenitors (marked with green dashed lines). Left panel: Control Lymph gland; right panel: Lymph gland with *ser* silencing at the Posterior Signaling Center. Single-plane confocal images of primary lobes from wandering third instar larvae are shown. Scale bars, 20 µm. Lower panel: quantification of the area occupied by *eater*-negative Core Progenitors. Error bars represent SD. *Antp* >, n = 14; *antp* > ser^{RNAi}, n =19.

(c) *Serrate*-expressing cells of the Posterior Signaling Center survive to genetic ablation of *antennapedia*-expressing cells. A*ntennapedia (antp)*-positive cells of the Posterior Signaling Center (PSC) are visualized with *antp*-Gal4 driven expression of GFP (*antp* > GFP, green), while *serrate* (*ser*) expressing cells are shown with anti-βGal staining (red) of *ser*-LacZ reporter. Expression of the pro-apoptotic protein Reaper (Rpr) with an *antp*-Gal4 driver from L2 stage onwards (see text) eliminates all *antp*-positive cells, but many *ser* expressing cells survive. Upper panels: control lymph glands without Rpr expression. The wild-type PSC comprises a mixed population of *antp* and *ser* double-positive cells (ser^+, $antp^+$) and *ser* positive-*antp* negative cells (ser^+, $antp^-$) (examples of the latter are shown with arrowheads); lower panels: lymph glands expressing Rpr under *antp*-Gal4. After genetic ablation, all of the observed PSC cells express *ser* and lack *antp* expression. Single-plane confocal images of the PSC region of primary lobes from wandering third instar larvae are shown. Scale bars, 20 µm.

664 **(d) After *antennapedia*-Gal4 driven genetic ablation, the abundance of the surviving *serrate*-**
665 **expressing cells of the Posterior Signaling Center correlates negatively with the amount of**
666 **Plasmatocytes.** In lymph glands in which *antp*-expressing cells of the Posterior Signaling Center
667 (PSC) have been ablated by *antp*-Gal4 driven expression of Reaper (Rpr), Plasmatocytes
668 differentiation (white, P1 staining) correlates negatively with the area occupied by *serrate*-LacZ
669 expressing cells that survived genetic ablation (red, βGal staining). Examples of large and small
670 *ser*-positive PSC areas are shown ("Large PSC" on the left panel and "Small PSC" on the right
671 panel, respectively). Inset shows a magnification of the PSC region, with all cells of the PSC
672 expressing *ser* but not *antp*. Whole Z-projection confocal images of primary lobes from
673 wandering third instar larvae are depicted. Scale bars, 20 µm. The graph shows quantification
674 of P1-positive area in *antp*-ablated lymph glands that exhibit large or small PSC area. PSC area
675 was considered small if it was less than %1.5 of the total lobe area). Large PSC, n = 7, Small
676 PSC, n = 8.
677
678
679 **Figure 4. Notch regulates the Plasmatocyte/Crystal Cell fate decision in Distal Progenitors.**
680 **(a) *Notch* (*N*) silencing in *domeMESO*-positive progenitors abolishes Crystal Cell specification**
681 **and promotes the Plasmatocyte cell fate.** *Notch* RNAi (N^{RNAi}) expression with the *domeMESO*-
682 Gal4 driver provoked loss of Crystal Cells (cyan: ProPO staining), along with increased
683 Plasmatocytes (red: P1 staining). Compare control lymph glands in upper panels with lymph
684 glands expressing N^{RNAi} in middle panels. Whole Z-projection confocal images of primary lobes
685 from wandering third instar larvae are displayed. Charts in lower panels show quantification of
686 the indicated markers (***p < 0.001). Error bars represent SD. *dome* >, n = 8; *dome* > N^{RNAi}, n =
687 8.
688 **(b) *Suppressor of hairless* (*su(H)*) silencing in *domeMESO*-positive progenitors is similar to**
689 ***notch* silencing.** *Su(H)* RNAi ($su(H)^{RNAi}$) expression with the *domeMESO*-Gal4 driver provoked
690 loss of Crystal Cells (cyan: ProPO staining) and increased Plasmatocytes (red: P1 staining).
691 Upper panels: control lymph glands; middle panels*:* lymph glands expressing $su(H)^{RNAi}$. Whole
692 Z-projection confocal images of primary lobes from wandering third instar larvae are shown.
693 Lower panels: quantification of the indicated markers (*p < 0.05, ***p < 0.001). Error bars
694 represent SD. *dome* >, n = 10; *dome* > $su(H)^{RNAi}$, n = 14.
695 **(c) Increased Notch activity in *domeMESO*-positive progenitors favors the Crystal Cell fate**
696 **and inhibits the Plasmatocyte fate.** Full-length Notch (Notch) or the Notch Intracellular
697 Domain (NICD) were over-expressed with a *domeMESO*-Gal4 driver. In the upper panels, a
698 control lymph gland is shown. In the rows below lymph glands overexpressing Notch (2nd row)
699 or NICD (3rd row) are shown. Whole Z-projection confocal images of primary lobes from
700 wandering third instar larvae are depicted. Bottom row: Quantification of the results. Different
701 letters indicate statistical difference (Tukey´s multiple comparison test). Error bars represent
702 SD. *dome* >, n = 6; *dome* > Notch, n = 6; *dome* > NICD, n = 4.
703 **(d) Over-expression of Suppressor of Hairless (Su(H)) in *domeMESO*-positive progenitors**
704 **provokes reduction of Plasmatocytes and increase of Crystal Cells, similarly to Notch over-**
705 **expression.** Plasmatocytes are visualized in red (P1 staining) and Crystal Cells in cyan (ProPO
706 staining). Upper panels: Control lymph glands; middle panels: Lymph glands with *domeMESO*-
707 Gal4 driven over-expression of Su(H). Whole Z-projection confocal images of primary lobes
708 from wandering third instar larvae are displayed. Scale bar, 20 µm. Lower panels:
709 Quantification of the results (***p < 0.001). Error bars represent SD. *dome* >, n = 7; *dome* >
710 Su(H), n = 8.
711

712 **Figure 5. Eater is an early Plasmatocyte fate marker in Distal Progenitors.**
713 **(a) Eater is expressed in all but a few Distal Progenitors of wandering 3rd instar lymph glands.**
714 Pictures show a magnification of the Region 2 of Fig. 1e, which corresponds to the Distal
715 Progenitor region that expresses the *domeMESO*-GFP reporter (green), but lacks *tepIV*-Gal4
716 driven BFP expression (*tepIV* > BFP, white). *Eater*-dsRed reporter (red) is expressed at high
717 levels in most of Distal Progenitors, with exception of a few cells that show reduced or null
718 levels (examples depicted with arrowheads). Single-plane confocal images of primary lobes
719 from wandering third instar larvae are shown. Scale bar, 10 µm.
720 **(b) In the Cortical Zone, the few differentiating cells that do not express *eater* are Crystal Cell**
721 **Progenitors.** Lozenge (Lz) staining (cyan) and *eater*-dsRed expression (red) is shown in lymph
722 glands that also express GFP under *hml*-Gal4 control (*hml* > GFP, green). Inset shows an
723 example of an *hml* > GFP positive cell that expresses the CC Progenitor marker Lz (white
724 arrowhead), and another example of a *hml* > GFP positive cell that expresses *eater*-dsRed
725 (yellow arrowhead). The Lz-expressing CC Progenitor lacks *eater*-dsRed expression (white
726 arrowhead). Single-plane confocal images of primary lobes from wandering third instar larvae
727 are shown. Scale bar, 20 µm.
728 **(c) *Eater* is never expressed during Crystal Cell development.** *Eater*-Gal4 driver was used to
729 express the G-TRACE system, which allows real time and lineage detection of the expression of
730 the Gal4 driver of interest. Crystal Cells are visualized with ProPO staining (cyan), and display
731 neither real time (RT exp., red) nor lineage expression (Lin exp., green) of the *eater*-Gal4 driver
732 (two examples are indicated by arrowheads). Single-plane confocal images of primary lobes
733 from wandering third instar larvae are shown. Scale bar, 20 µm.
734 **(d) Notch regulates *Eater* expression in *domeMESO*-positive cells.** *Eater*-dsRed reporter
735 expression (red) is shown for control lymph glands (upper panels), and for lymph glands with
736 *domeMESO*-Gal4 driven over-expression of Notch (2nd row panels) or *domeMESO*-Gal4 driven
737 silencing of *notch* (3rd row panels). *DomeMESO*-positive cells are shown by *domeMESO*-Gal4
738 driven expression of GFP (*domeMESO* > GFP, green). Notch over-expression with *domeMESO*-
739 Gal4 dramatically reduces *eater*-dsRed expression in all *domeMESO*-positive cells, while *notch*
740 RNAi (N^{RNAi}) expression with *domeMESO*-Gal4 provokes that all *domeMESO*-positive cells
741 express *eater*-dsRed. Single-plane confocal images of primary lobes from wandering third
742 instar larvae are shown. Scale bar, 20 µm. Lower panel: Quantification of double positive
743 $dome^+$, $eater^+$ cells in control and Notch over-expressing lymph glands (***$p < 0.001$). Error
744 bars represent SD. *Dome* >, n = 9; *dome* > Notch, n = 9.
745
746
747 **Figure 6. Serrate expressed at the MZ/CZ boundary regulates the Plasmatocyte/Crystal Cell**
748 **fate in Decision Progenitors.**
749 **(a) A fraction of s*er*-expressing cells at the MZ/CZ boundary expresses *domeMESO*.** *Ser*-
750 positive cells are visualized with βGal staining (red) of the *ser*-LacZ reporter. *DomeMESO-Gal4*
751 driver expression of GFP (*domeMESO* > GFP, green) is observed in a proportion of *ser*-
752 expressing cells at the MZ/CZ boundary (examples are shown with arrowheads). The yellow
753 dashed line marks the Posterior Signaling Center area. On the right, a magnification of this area
754 shows that *ser* is also expressed in these cells, but in this case *domeMESO* is not co-expressed.
755 Single-plane confocal images of a primary lymph gland lobe from mid-3rd instar larvae are
756 shown. Scale bar, 20 µm.
757 **(b) Serrate (Ser) at the Medullary Zone is required for Crystal Cell differentiation and**
758 **Plasmatocyte fate inhibition.** Plasmatocytes are visualized in red (P1 staining) and Crystal Cells
759 in cyan (ProPO staining), in control lymph glands (upper panels) and in lymph glands that

760 express a *ser* RNAi (*ser*^{RNAi}) under *domeMESO*-Gal4 driver control (middle panels). Whole Z-
761 project confocal images of primary lobes from wandering third instar larvae are shown. Scale
762 bar, 20 µm. Lower panels: Quantification of the results (***p < 0.001). Error bars represent SD.
763 *dome* >, n = 10; *dome* > *ser*^{RNAi}, n = 12.
764 **(c) Over-expression of Serrate (Ser) at the Medullary Zone provokes an increase in Crystal**
765 **Cell numbers and a reduction in Plasmatocyte differentiation.** Pictures show Plasmatocytes
766 (red, P1 staining) and Crystal Cells (cyan, ProPO staining) in control lymph glands (upper
767 panels) and in lymph glands with *domeMESO*-Gal4 driven Ser over-expression (middle panels).
768 Whole Z-project confocal images of primary lobes from wandering third instar larvae are
769 shown. Scale bar, 20 µm. Lower panels: Quantification of the results (***p < 0.001). Error bars
770 represent SD. *Dome* >, n = 12; *dome* > Ser, n = 12.
771 **(d) Neuralized (Neu) at the Medullary Zone is required for Crystal Cell differentiation and**
772 **Plasmatocyte fate inhibition.** Plasmatocytes (red, P1 staining) and Crystal Cells (cyan, ProPO
773 staining) is shown in control lymph glands (upper panels) and in lymph glands with *neu* RNAi
774 (*neu*^{RNAi}) expression under *domeMESO*-Gal4 driver control (middle panels). Whole Z-project
775 confocal images of primary lobes from wandering third instar larvae are shown. Scale bar, 20
776 µm. Lower panels: Quantification of the indicated markers (***p < 0.001). Error bars represent
777 SD. *Dome* >, n = 10; *dome* > *neu*^{RNAi}, n = 10.
778
779
780 **Figure 7. Model showing the redefinition of progenitor populations and the functions of the**
781 **Notch pathway.** In *tepIV*$^{+}$*, dome*$^{+}$ Core Progenitors (dark green) Notch is activated by its ligand
782 Ser (Ser), expressed at Posterior Signaling Center (PSC) cells. This Notch activation is required
783 to avoid premature Core Progenitor differentiation towards both the Plasmatocyte (PL) and
784 Crystal Cell fate (CC) (upper and lower rows of cells, respectively). Thereafter *tepIV* expression
785 ceases, while *dome* expression continues, defining a second population of progenitors, the
786 Distal Progenitors (light green). Early Distal Progenitors do not express any differentiation
787 marker, and constitute the stage where a cell fate decision between the Plasmatocyte and the
788 Crystal Cell fate is made. This cell fate decision also depends on Notch, which is activated by
789 Ser expressed at the MZ/CZ boundary. Notch activation in Distal Progenitors induces CC
790 differentiation and inhibits the PL fate. Without contact from Ser-expressing cells, Distal
791 Progenitors follow a default PL differentiation program. This early fate decision is evidenced
792 later in development by the expression of *dome* and *eater* in Distal Progenitors destined to a
793 PL fate (*eater* expression is represented with a dark red outline), while Distal Progenitors
794 destined to CCs lack *eater* expression. Once blood cells start expressing *hemolectin* at the
795 Cortical Zone (*hml,* pink), they are already committed either to a PL or to a CC fate. Cells
796 committed to a PL fate continue expressing *eater,* while cells committed to become CCs now
797 express Lozenge (Lz, light blue). Finally, mature PLs co-express *eater*, *hml* and the P1-antigen
798 (red); while mature CCs co-express Lz and ProPO (dark blue) but have ended *hml* expression.

Supplementary Figure 1

a

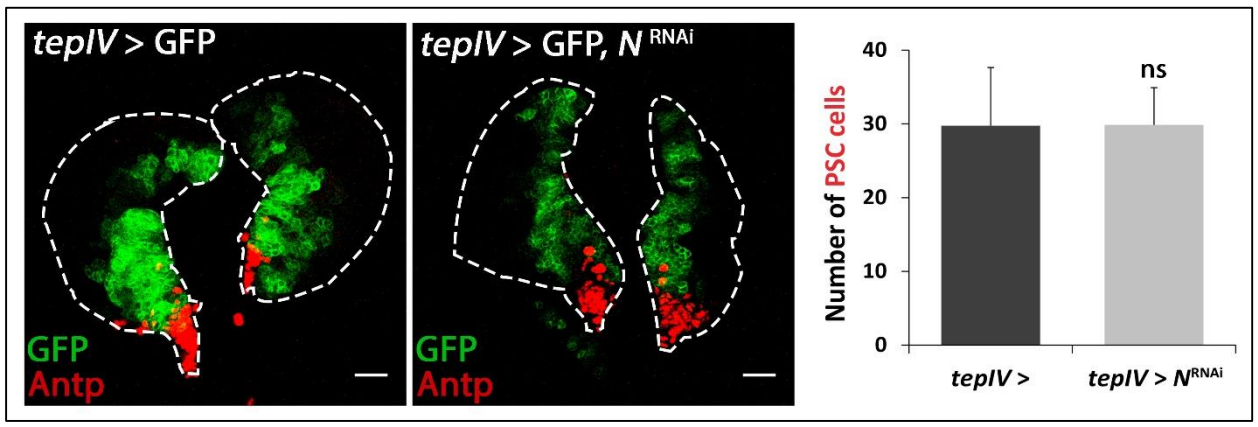

b

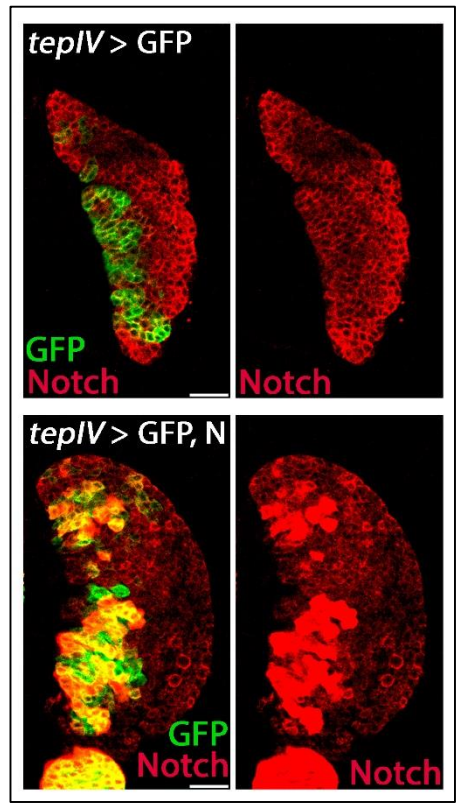

c

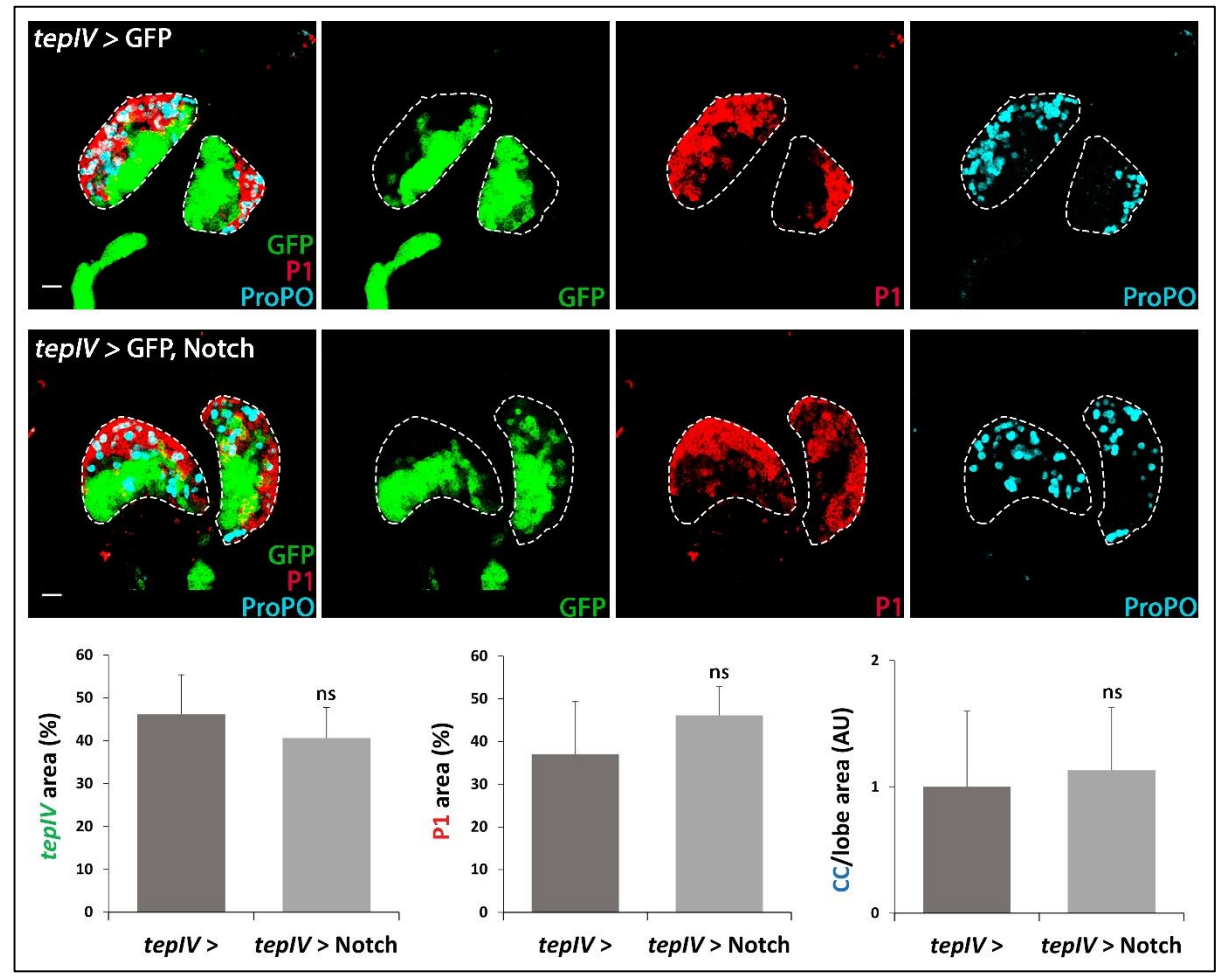

d

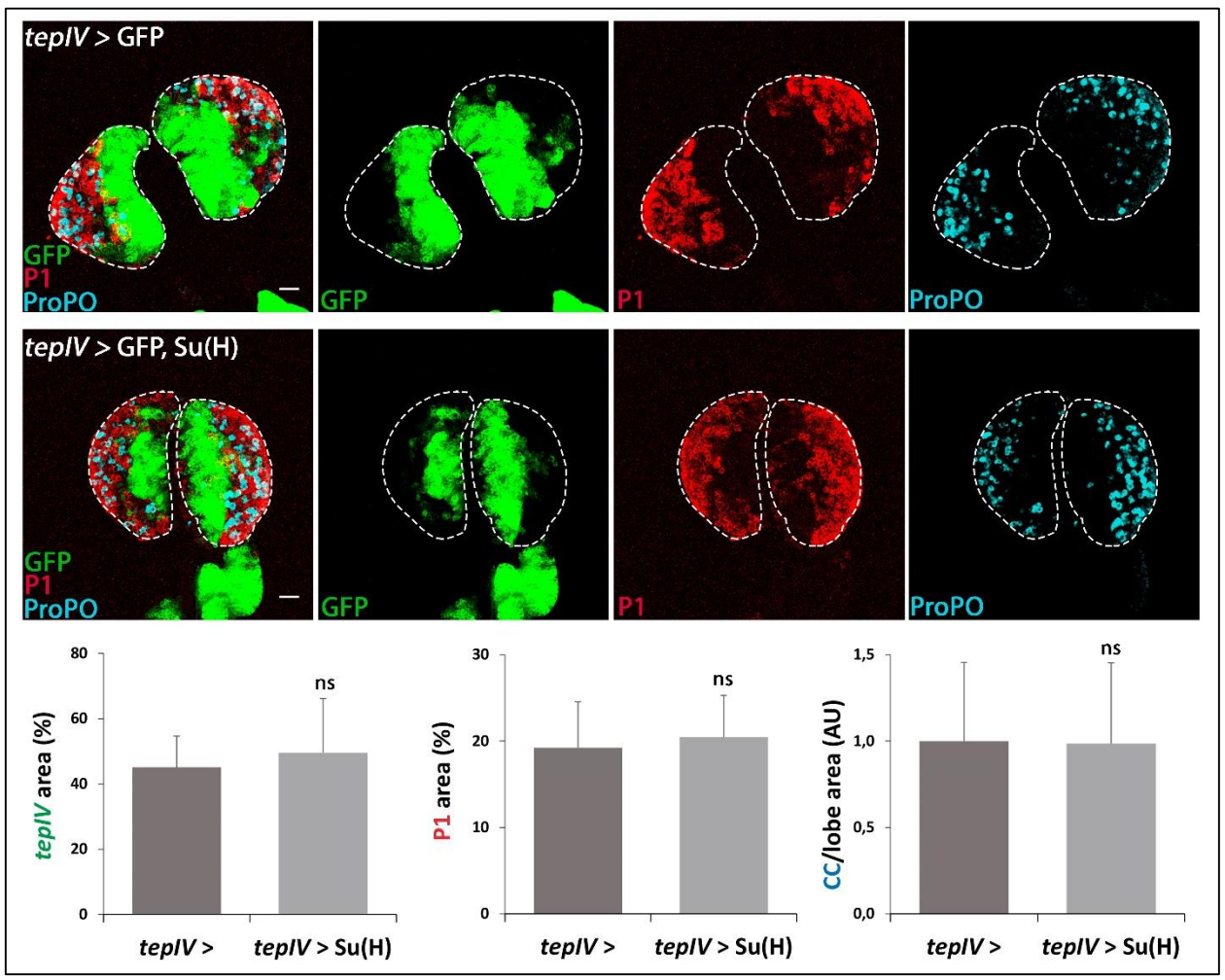

e

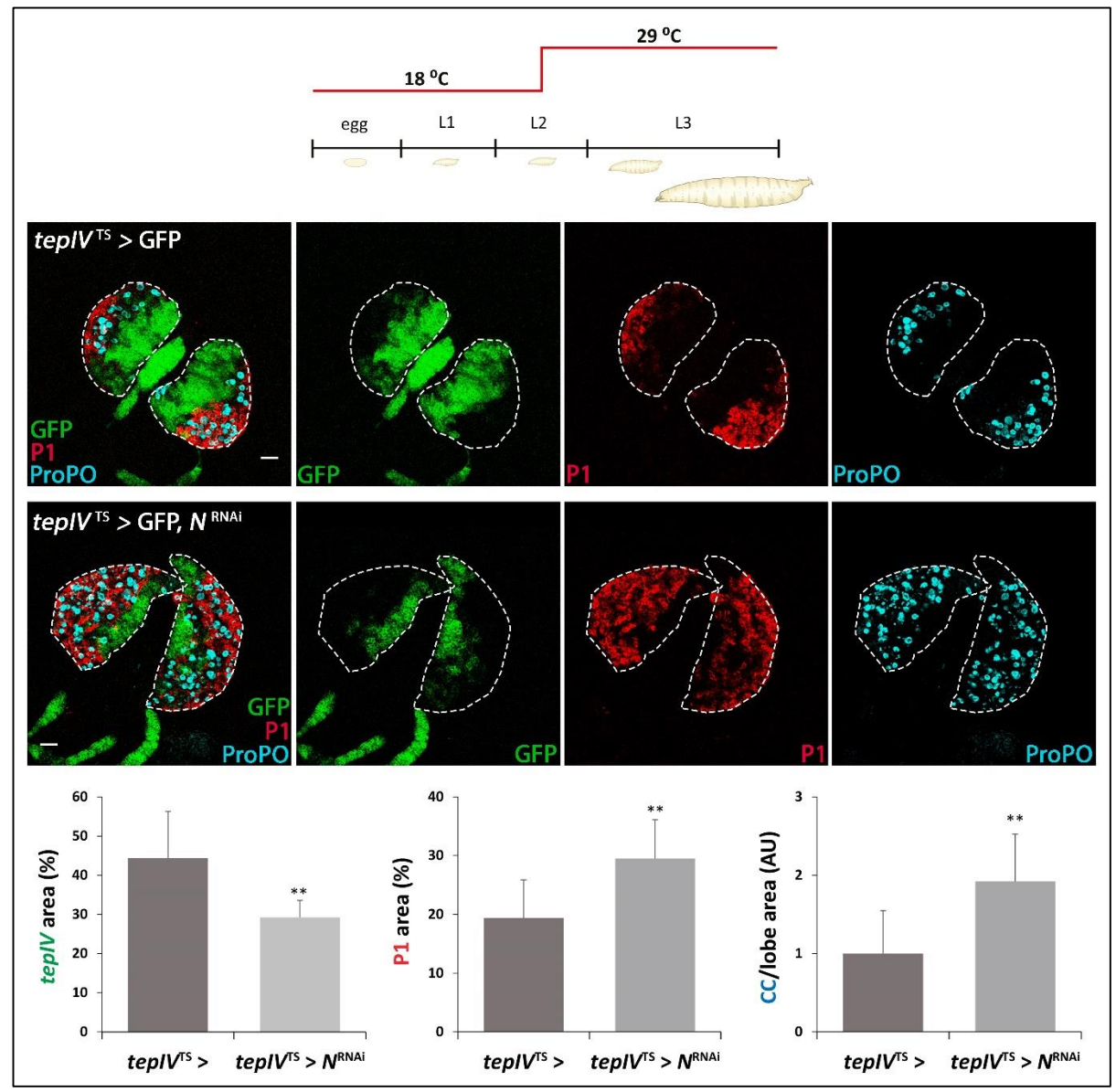

Supplementary Figure 2

a

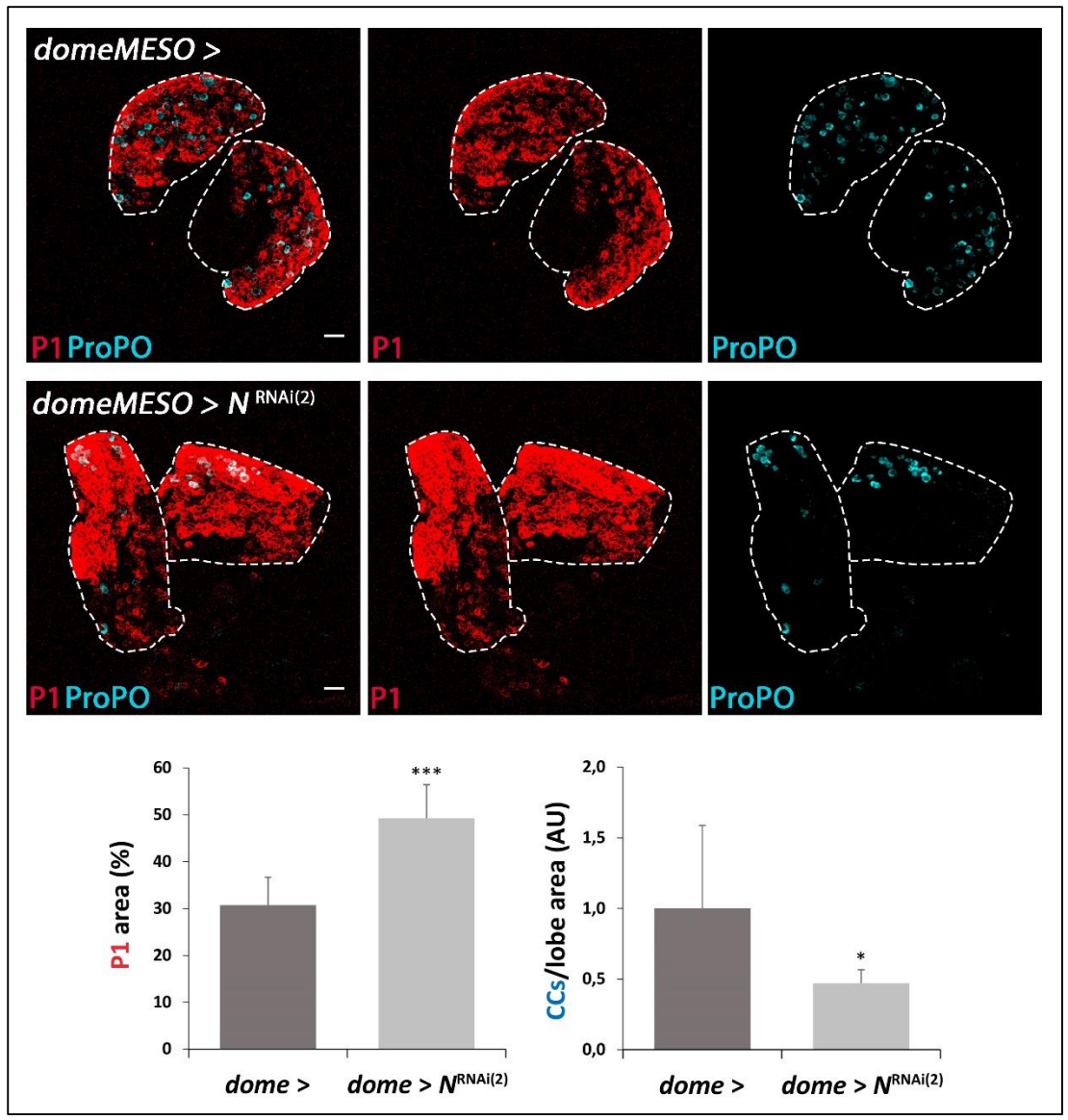

b

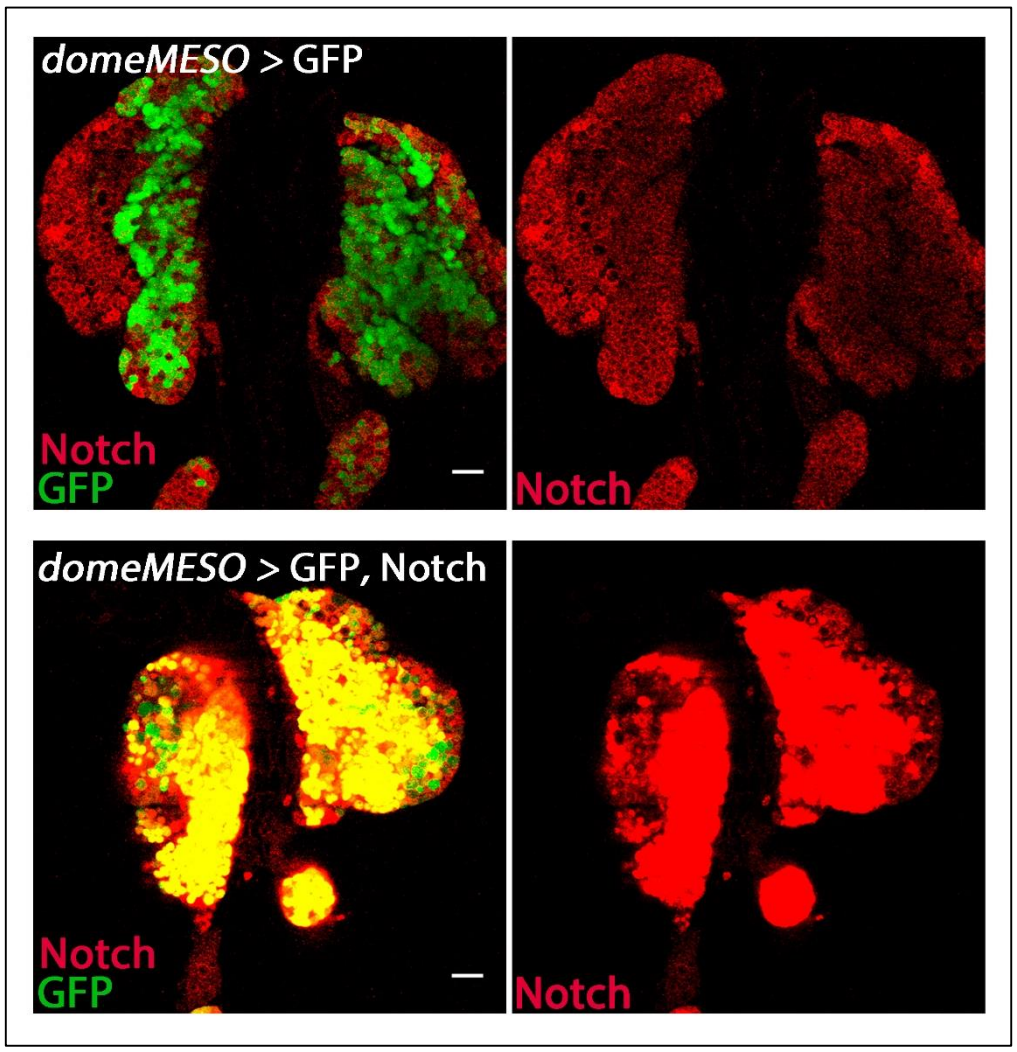

c

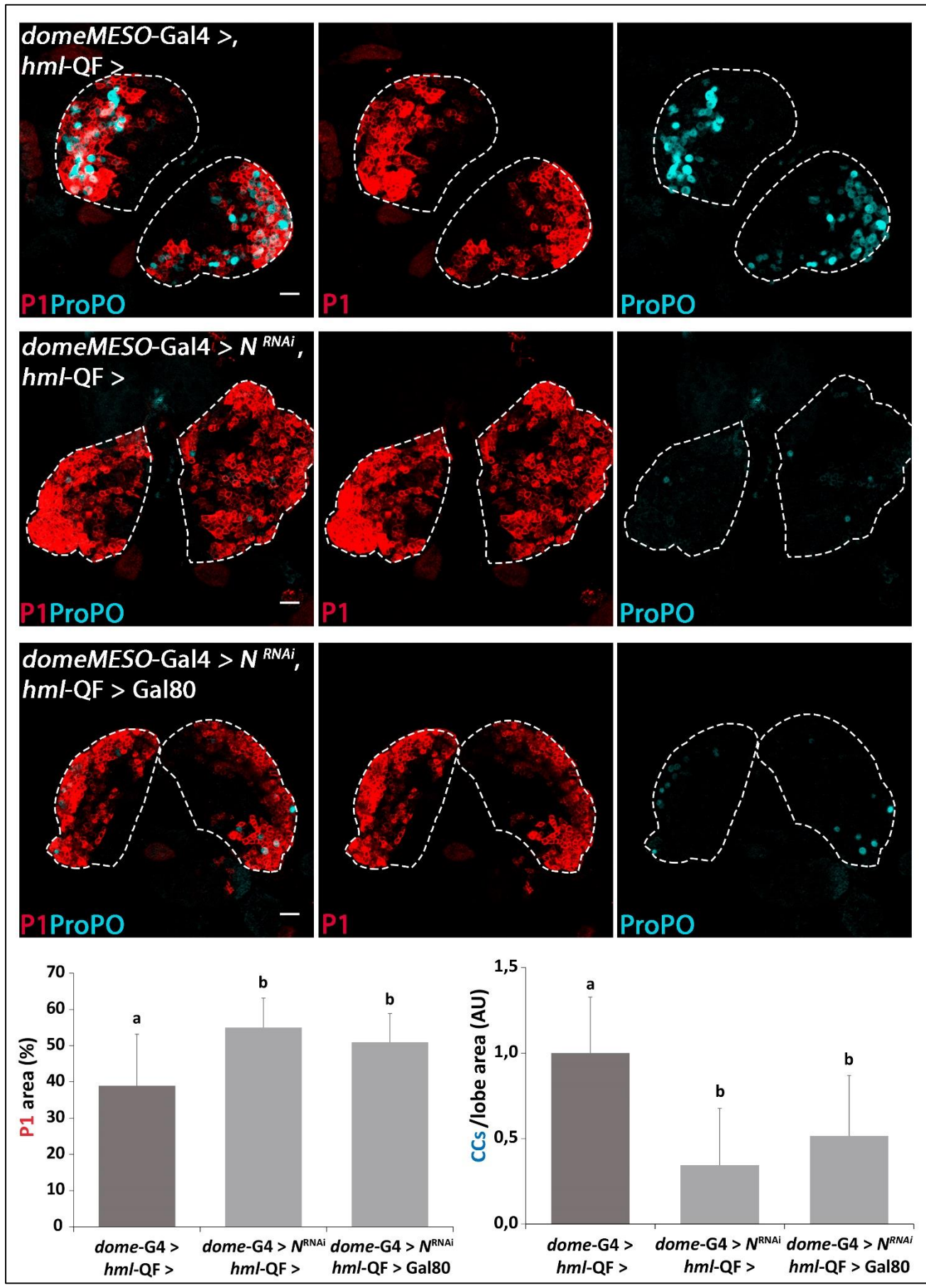

d

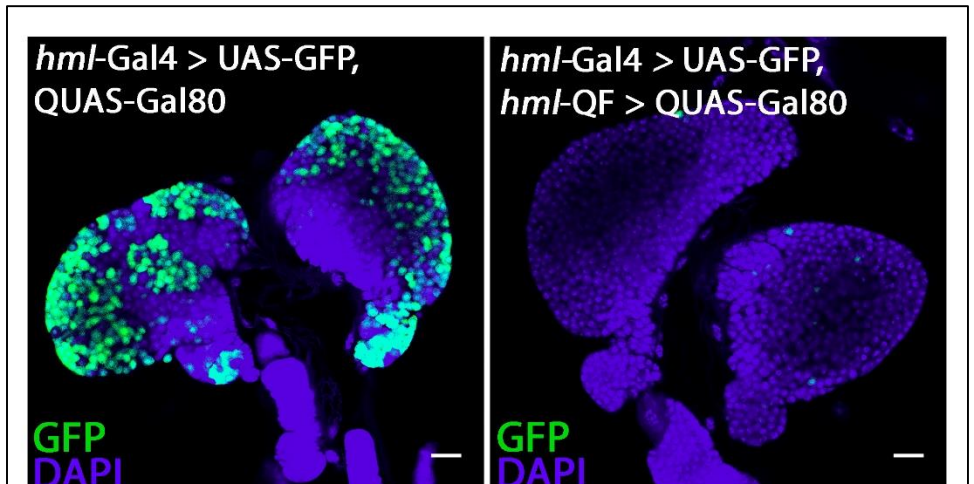

Supplementary Figure 3

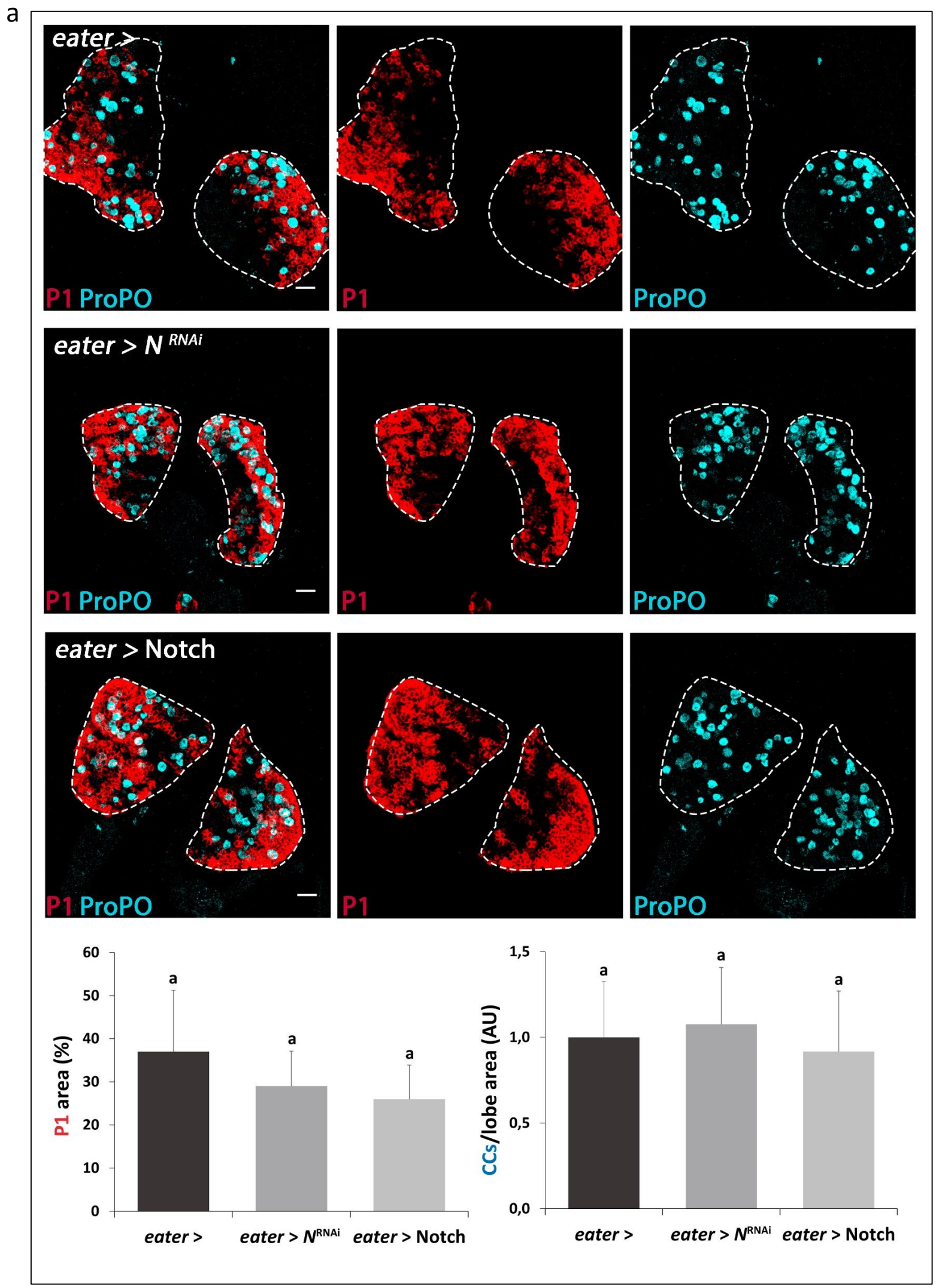

Supplementary Figure legends

Figure S1.

(a) *Notch* silencing in Core Progenitors does not affect the size of the Posterior Signaling Center. *TepIV*-Gal4 driven expression of a *notch* RNAi (N^{RNAi}), does not affect the number of Posterior Signaling Center cells, as shown by an anti-Antennapedia (Antp) staining (red). *TepIV* > GFP expression (green) labels Core Progenitors. Left panel: Control lymph gland without RNAi expression; central panel: Lymph gland that expresses N^{RNAi} driven by *tepIV*-Gal4. Single-plane confocal images of primary lobes from wandering third instar larvae are shown. Scale bars, 20 µm. Right panel: Quantification of the number of Posterior Signaling Center cells per lobe (ns: Non-significant). Error bars represent SD. *tepIV* >, n = 8; *tepIV* > N^{RNAi}, n = 8.

(b) Notch over-expression in Core Progenitors. Anti-Notch (N) staining (red) was utilized to demonstrate an increase of Notch levels in Core Progenitors following *tepIV*-Gal4 driven over-expression of full-length Notch. Core progenitors are visualized in green (*tepIV* > GFP). Upper panel: Control lymph glands; lower panel: lymph glands that over-express Notch. Single-plane confocal images of primary lobes from wandering third instar larvae are shown. Scale bars, 20 µm.

(c-d) Over-expression of Notch (d) or Supressor of Hairless (e) in Core Progenitors has no effect on cell differentiation. Core Progenitors are visualized in green (*tepIV* > GFP); Plasmatocytes in red (P1 staining); and Crystal Cells in cyan (ProPO staining). Upper panels: Control lymph glands; middle panels: Lymph glands with *tepIV*-Gal4 driven over-expression of full-length Notch (d) or Su(H) (e). Whole Z-projection confocal images of primary lobes from wandering third instar larvae are shown. Scale bar, 20 µm. Lower panels: Quantification of the results (ns: Non-significant). Error bars represent SD. *tepIV* >, n = 8; *tepIV* > Notch, n = 8; *tepIV* > Su(H), n = 8.

(e) Notch is not required for Core Progenitor maintenance at L1 larval stage. *Notch* (*N*) silencing was induced in Core Progenitors from mid L2 stage onwards using the *tub*-Gal80^{ts}, *tepIV*-Gal4 genetic combination ($tepIV^{TS}$), leading to Core Progenitor loss (green: *tepIV* > GFP), and enhanced differentiation of Plasmatocytes (red: P1 staining) and Crystal Cells (cyan: ProPO staining). Top: temperature protocol utilized in the experiment. Upper panels: control lymph glands without RNAi expression; middle panels: Lymph glands expressing N^{RNAi}. Whole Z-projection confocal images of wandering third instar larvae are shown. Scale bars, 20 µm. Lower panels: Quantification of the results (**p < 0.01). Error bars represent SD. $tepIV^{TS}$>, n = 9; $tepIV^{TS}$>N^{RNAi}, n = 10.

Figure S2.

(a) *Notch* silencing with the *domeMESO*-Gal4 driver, utilizing an alternative *notch* RNAi construct ($N^{RNAi(2)}$), also provoked increase of Plasmatocytes and reduction of Crystal Cells. Plasmatocytes are visualized in red (P1 staining) and Crystal Cells in cyan (ProPO staining). Upper panels: Control lymph glands; middle panels: Lymph glands with expression of a $N^{RNAi(2)}$ construct with a different target sequence than the N^{RNAi} used in Fig. 4a. Whole Z-projection confocal images of primary lobes from wandering third instar larvae are shown. Scale bar, 20 µm. Lower panels: Quantification of the results (*p < 0.05, ***p < 0.001). Error bars represent SD. *dome* >, n = 8; *dome* > $N^{RNAi(2)}$, n = 5.

(b) Notch over-expression in *domeMESO*-positive progenitors. Anti-Notch (N) staining (red) was utilized to demonstrate an increase of Notch levels in progenitors (visualized in green; *domeMESO* > GFP) following *domeMESO*-Gal4 driven over-expression of full-length Notch.

846 Upper panel: Control lymph glands; lower panel: lymph glands that over-express Notch. Single-
847 plane confocal images of primary lobes from wandering third instar larvae are shown. Scale
848 bars, 20 µm.
849 **(c) *Notch* silencing in *domeMESO*-positive progenitors which do not express *hemolectin* (*hml*)**
850 **recapitulates increase of Plasmatocytes and reduction of Crystal Cells.** *Notch* RNAi (N^{RNAi}) was
851 expressed with the *domeMESO*-Gal4 driver, together or not with the Gal4 inhibitor Gal80 in
852 *hml*-positive cells (achieved through *hml*-QF driven expression of QUAS-Gal80). Plasmatocytes
853 are visualized in red (P1 staining) and Crystal Cells in cyan (ProPO staining). Upper panels:
854 control lymph glands not expressing N^{RNAi}; 2nd row panels: lymph glands expressing N^{RNAi},
855 without Gal80 expression; 3rd row panels: lymph glands expressing N^{RNAi}, with Gal80 expression
856 in *hml*-positive cells. Whole Z-projection confocal images of primary lobes from wandering
857 third instar larvae are shown. Scale bar, 20 µm. Lower panels: Quantification of the indicated
858 markers. The letters indicate statistical difference (Tukey´s multiple comparison test). Error
859 bars represent SD. *Dome*-G4 >, *hml*-QF >, n = 10; *dome*-G4 > N^{RNAi} , *hml*-QF >, n = 10; *dome*-G4
860 > N^{RNAi} , *hml*-QF > Gal80, n = 14.
861 **(d) *Hml*-QF driven expression of QUAS-Gal80 is effective in repressing Gal4 activity at the**
862 **Cortical Zone.** Gal80 is effective in inhibiting Gal4 activity, as assessed by a virtual block of *hml*-
863 Gal4 driven UAS-GFP expression (green) when Gal80 is expressed in the same cells using *hml*-
864 QF > QUAS-Gal80 (right panel). Left panel: control lymph glands without expression of Gal80.
865 DAPI staining shows nuclei. Single-plane confocal images of wandering third instar primary
866 lymph gland lobes are shown. Scale bars, 20 µm.
867
868
869 **Figure S3.**
870 **(a) Notch does not affect Plasmatocyte or Crystal Cell differentiation after *eater* expression is**
871 **initiated.** Pictures show expression of the Plasmatocyte marker P1 (red) and the Crystal Cell
872 marker ProPO (cyan) in control lymph glands (upper panels) and in lymph glands with *eater*-
873 Gal4 driven expression of *notch* RNAi (2nd row panels) or full-length Notch (3rd row panels).
874 Whole Z-projection confocal images of primary lobes from wandering third instar larvae are
875 depicted. Scale bar, 20 µm. Lower panels: Quantification of the indicated markers. Same letter
876 indicates no statistical difference between means (Tukey´s multiple comparison test). *Eater* >,
877 n = 8; *eater* > N^{RNAi}, n = 10; *eater* > Notch, n = 10.